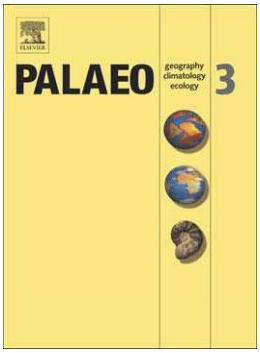

Rhodoliths, uniformitarianism, and Darwin: Pleistocene and Recent carbonate deposits in the Cape Verde and Canary archipelagos

Markes E. Johnson, B. Gudveig Baarli, Mário Cachão, Carlos M. da Silva, Jorge Ledesma-Vázquez, Eduardo J. Mayoral, Ricardo S. Ramalho, Ana Santos

PII: S0031-0182(12)00092-2
DOI: doi: 10.1016/j.palaeo.2012.02.019
Reference: PALAEO 6048

To appear in: *Palaeogeography, Palaeoclimatology, Palaeoecology*

Received date: 9 December 2011
Revised date: 10 February 2012
Accepted date: 14 February 2012

Please cite this article as: Johnson, Markes E., Baarli, B. Gudveig, Cachão, Mário, da Silva, Carlos M., Ledesma-Vázquez, Jorge, Mayoral, Eduardo J., Ramalho, Ricardo S., Santos, Ana, Rhodoliths, uniformitarianism, and Darwin: Pleistocene and Recent carbonate deposits in the Cape Verde and Canary archipelagos, *Palaeogeography, Palaeoclimatology, Palaeoecology* (2012), doi: 10.1016/j.palaeo.2012.02.019

Palaeogeography, Palaeoclimatology, Palaeoecology

Rhodoliths, uniformitarianism, and Darwin: Pleistocene and Recent carbonate deposits in the Cape Verde and Canary archipelagos

Markes E. Johnson[a]*, B. Gudveig Baarli[a], Mário Cachão[b], Carlos M. da Silva[b], Jorge Ledesma-Vázquez[c], Eduardo J. Mayoral[d], Ricardo S. Ramalho[e] and Ana Santos[d]

[a] *Department of Geosciences, Williams College, Williamstown, MA 01267 USA*

[b] *Faculdade de Ciências da Universidade de Lisboa, Departamento de Geologia e Centro de Geologia, Campo Grande, 1749-016 Lisboa, Portugal*

[c] *Facultad de Ciencias Marinas, Universidad Autónoma de Baja California, Ensenada, BC 22800, México*

[d] *Departamento de Geodinámica y Paleontología, Facultad de Ciencias Experimentales, Universidad de Huelva, Campus de El Carmen, Avda. 3 de Marzo, s/n, 21071 Huelva, Spain*

[e] *Institut für Geophysik, Westphälishe-Wilhelms Universitat, Corrensstraße 24, 48149 Münster, Germany*

* Corresponding author; E-mail address: mjohnson@williams.edu

ABSTRACT

Visiting “St. Jago” (Santiago) in the Cape Verde Islands in 1832 and again in 1836 aboard HMS *Beagle*, Charles Darwin was the first to trace and describe the tri-part sequence of white limestone and sandstone beds stratigraphically located between two

levels of basalt exposed almost uninterrupted for 10 km along coastal cliffs. The Pleistocene carbonate sediments dominated by rhodoliths and rhodolith debris accumulated on a basalt shelf and subsequently became buried by subaerial and submarine basalt on the southeast coastline of Santiago. The main goal of this contribution is to re-examine Darwin's stratigraphic sequence. The secondary goal is to provide a general taphonomical model based on the observation of Recent rhodolith deposits for evaluation of fossil rhodolith assemblages. Environmental uniformitarianism is employed to understand the depositional history of the southern Santiago rhodolith-bearing strata. The mixed clastic-carbonate sequence includes a basalt-derived basal conglomerate with an intertidal to shallow subtidal fossil assemblage mainly denoted by limpets and oysters. Upper layers typically demonstrate swaley and hummocky cross stratification incorporating rhodolith debris further modified by bioturbation. Pillow basalts from 10 – 18 m in thickness succeeded by subaerial flows imply swift burial of the carbonate succession under equivalent water depths. The calcareous nannofossil assemblage was investigated to more precisely date the deposits. Darwin's paleoshore is reinterpreted to represent two different transgressions occurring between approximately 1.1 and 0.7 Ma. Taphonomic grades from whole rhodoliths to finely crushed rhodolith debris observed under present-day conditions on Maio (Cape Verde Islands) and Fuerteventura (Canary Islands) were used to model rhodolith preservation and to constrain the depositional settings to which rhodoliths may be transported from the offshore banks where they naturally thrive. Coastward transport of rhodoliths commonly ends with deposition in subtidal storm beds, tidal pools, and platform over-wash deposits, as well as beach, berm, hurricane, tsunami, and coastal dune deposits.

Highlights

- Darwin posited a Tertiary age for basalt-limestone-basalt layers.
- Nannofossils, indicate a Pleistocene age (1.1 - 0.7 Ma).
- Darwin recognized marine onlap on a former rocky shore, but not the uneven surface related to drowned headlands.
- Darwin identified one paleoshore. Two paleoshores are distinguished by overlying subaerial flows vs. pillow basalts.
- Darwin identified fossil Nulliporae (coralline red algae). Shape analysis shows selection for transported forms.
- Rhodolith taphonomy from modern coastal deposits (Maio and Fuerteventura) aids interpretation of fossil deposits.

Keywords: Coastal paleotopography, Rhodoliths (Rhodophyta), Taphonomy, Swaley and hummocky cross-stratification, Volcanic islands, Cape Verde Islands (Santiago and Maio), Canary Islands (Fuerteventura)

1. Introduction

The principal island of "St. Jago" (Santiago) in the Cape Verde archipelago off the northwest shores of Africa was one of the few destinations Charles Darwin revisited during his five-year circumnavigation of the world aboard HMS *Beagle*. As revealed in his autobiography (Darwin, 1958), the 22-year-old naturalist was inspired during the initial visit from January 16 to February 8 in 1832 to plan a book on the geology of volcanic islands. The object of his inspiration was a 10-km stretch of coastline that included "Quail Island" (Ilhéu de Santa Maria) in the harbor of the provincial capital "Praya" (Cidade da Praia). Darwin explored the harbor island and surrounding coastal region in substantial detail, following a horizontal white band of calcareous matter resting on basalt and overlain by basalt flows (Darwin, 1839). The several years between publication of his popular account of the 1831–1836 voyage (Darwin, 1839) and his

observations on volcanic islands (Darwin, 1844), resulted in a much-expanded text regarding the phenomena of the Praia sea cliffs.

In a single paragraph from Darwin's 1839 account, the distinctive calcareous layer was attributed to fossil seashells, most examples of which he found to be extant on adjacent beaches. In the expanded 1844 version, the 6-m thick calcareous deposit was reappraised to include abundant fossil "Nulliporae" indicative of algal affinities, as well as extensive debris likened in appearance to "mortar." At least a dozen of the fossil algal concretions collected by Darwin still reside in a drawer at the Sedgwick Museum, Cambridge University (Herbert, 2005, figs. 5.5 and 5.6). These historical specimens clearly are fossil rhodoliths. In today's nomenclature, the spherical growths represent free-living nodules made up of nongeniculate coralline red algae (Division Rhodophyta). The mortar to which Darwin referred, is indicative of copious debris derived from rhodolith fragmentation and sand from eroded basalt.

Only three weeks into the voyage when HMS *Beagle* arrived in the Cape Verde Islands, Darwin had with him a copy of the first volume by Lyell (1830) on uniformitarian patterns in the Recent and geological record. Although Darwin clearly adopted a gradualist viewpoint on geology later in the voyage, it appears that the philosophy of Lyell (1830) had yet to make an impression. Pearson and Nicholas (2007) present convincing evidence that Darwin's observations on the island's geology were initially constrained by a catastrophist outlook more prevalent at the time. Gradual uplift and subsidence of the earth's crust is one of the essential uniformitarian themes of Lyell's geology, a lesson that Darwin (1842) mastered in his analysis of coral atolls related to the sinking of volcanic islands in the southern Pacific and Indian oceans. By the time

Darwin returned to Santiago Island near the end of the voyage in 1836, he had seen much of the world and was prepared to review the tri-part sequence of basalt, limestone, and basalt from a different perspective.

The unattached coralline red algae that grow as rhodoliths thrive today on banks small and large in all seas and oceans across a wide range of tropical to polar climates (Foster, 2001). An extensive fossil record of rhodoliths can be traced back to the Early Cretaceous (Aguirre et al., 2010). The rhodalgal habitat is considered to have achieved maximum global domination as a carbonate facies during the Middle Miocene at about 15 Ma, before undergoing a decline concomitant with resurgence of the hermatypic-coral habitat during the later Neogene (Halfar and Mutti, 2005). Given the breath of studies on present-day and fossil rhodoliths from many parts of the world including Brazil (Pereira Filho et al., 2012; Dias and Villaça 2012), Japan (Bassi et al., 2009; Matsuda and Iryu, 2011), New Zealand (Basso et al., 2009; Nalin et al. 2008), Mexico (Steller et al., 2009; Johnson et al. 2009), and Mediterranean area (Basso, 1998; Bassi and Nebelsick, 2010), it is surprising no one has revisited the classic ground first covered by Charles Darwin 180 years ago with specific regard to the rhodolith deposits on Santiago Island.

The main goal of this contribution is to re-examine Darwin's rhodolith sequence from southeastern Santiago Island in the framework of its defining unconformities within the main volcanostratigraphic units defined by Serralheiro (1976). Multiple techniques of stratigraphic analysis are applied to the succession for the first time. As an application of environmental uniformitarianism, additional insight on strata from the Praia sea cliffs on Santiago was aided through comparisons to present-day coastal deposits that feature extensive rhodoliths and rhodolith debris on Maio (Cape Verde Islands) and

Fuerteventura (Canary Islands). Thus, a secondary goal is to provide examples of taphonomic grades in contemporary rhodolith deposits for evaluation of rock formations bearing conspicuous rhodolith content, regardless of geologic age.

2. Geographic and geologic settings

2.1 Physical geography

Persistent trade winds that reach Santiago Island from the northeast represent a critical physical trait that Darwin (1839, 1844) made explicit in his commentary. The same winds on Fuerteventura, second largest island in the Canary archipelago, are no less significant. In relation to their surrounding bathymetry, the size and shape of these islands control where living rhodolith banks may or may not develop on the seabed. In the case of Santiago and Maio islands (Fig. 1B), the south and southeastern shelves above a depth of 75 m delimit a constricted but highly suitable habitat where long-shore currents and wave refraction in clear waters contribute to the gentle circumrotary movement of rhodoliths to promote equitable photosynthesis. Where water energy is more vigorous, as for example under ocean swells on north and northeastern coasts (Fig. 1B), physical abrasion and destruction of rhodoliths would be the expected result.

A similar constriction of shelf space above the 75-m isobath on the eastern and southeastern shelves of Fuerteventura (Canary Islands) is evident, where long-shore currents and wave refraction is advantageous to the potential development of living rhodolith banks (Figs. 2A, B). In addition, a more commodious bank is located off the north coast of Fuerteventura across from Isla Lanzarote, as defined by the Bocina Channel (Fig. 2C). Situated 2 km off the northeast shores of Fuerteventura and 8 km off

southwestern Lanzarote, tiny Isla de Lobos (468 hectares) is noted for its historically lucrative lime industry, which exploited fossil rhodolith deposits and enormous quantities of Recent rhodoliths stranded on beaches within sheltered bays. The extensive bank in this region is subject to seabed re-working that is perhaps less destabilizing in the leeward shelter of Isla Lanzarote. Fossil and contemporary rhodolith deposits occur extensively along the shores of Fuerteventura. Modern maërl beds mixed with sand are recorded around all margins of Fuerteventura based on studies by the Atlantic Environmental Research Center at La Laguna University in Tenerife (Óscar Monterroso Hoyos, personal communication, February 8, 2012).

2.2 History of volcanism and magnetic reversals

The islands of the Canary and Cape Verde archipelagos are volcanic in origin as a result of magmatic hot-spot activity associated with mantle melting and melt extraction to the surface on the northwest margin of the African plate (Carracedo et al., 1998; Holm et al., 2008). Although the various islands of the Canary archipelago (7,500 km^2) are nearly twice the size in total area compared to those in the Cape Verde archipelago (4,000 km^2), the latter sit atop a notably large seafloor anomaly called the Cape Verde Rise. Fogo Island in the southwest part of the archipelago (Fig. 1B) is Cape Verde's only active volcano, erupting as late as 1995. Some of the Canary Islands, including Tenerife, La Palma, and El Hierro in that archipelago (Fig. 2A) have historical records of eruption, but only El Hierro has shown recent seismic and volcanic activity.

Oceanic volcanoes go through several stages of development including the formation of a basement complex that sometimes incorporates uplifted sections of the sea

floor, an intermittent shield-building stage, and a post-erosional stage (Ramalho et al. 2010a). Fuerteventura is the oldest of the Canary Islands, with a foundation of gabbro, syenite, and carbonatite rocks that date to 20.6 Ma (Carracedo et al., 1998; Gutiérrez et al., 2006) together with integrated Jurassic to Cretaceous sea-floor sediments (Steiner et al., 1998). The shield-building stage on Fuerteventura commenced about 17 –16 Ma and concluded at approximately 9 Ma (Carracedo et al., 1998). Post-erosional volcanism has occurred sporadically on Fuerteventura over the last 5 m.y. Maio in the Cape Verde archipelago has a volcanic history similar in timing to that of Fuerteventura (Ramalho et al., 2010a and references therein) that integrates Jurassic and Cretaceous sea-floor sediments (Robertson, 1984). By comparison, Santiago is a much younger island with a foundational stage that dates from about 11 – 7 Ma; a shield-building stage that dates overall from 5 – 2.2 Ma; and a post-erosional stage within the last million years (Holm et al., 2008; Barker et al., 2010; Ramalho et al., 2010a).

Serralheiro (1976) produced a detailed geological map of Santiago, drawing distinctions between the Old Eruptive Complex, Flamengos Formation, Orgãos Formation, Pico da Antónia Eruptive Complex, Assomada Formation and Monte das Vacas Formation. The Old Eruptive Complex signifies the early foundational stage, which includes gabbro, phonolite, syenite, and carbonatite rocks (Barker et al., 2010). Distributed mainly in the central part of the island, the Flamengos Formation represents an early phase of shield building, entirely submarine, constrained to dates between 3.9 – 4.6 Ma (Barker et al., 2009, 2010; Ramalho et al. 2010b), whereas the more widely spread Pico da Antónia Eruptive Complex denotes a subsequent, mostly subaerial shield-building phase. This complex includes a lower member composed of thick pillow lavas

dated as old as 3.25 ± 0.05 Ma and an upper member with both subaqueous and subaerial flows dated not younger than 2.19 ± 0.12 Ma (Holm et al., 2008, table 2). Additional radiometric dates and chronostratigraphic analysis of the Pico da Antónia Eruptive Complex based on a 150-m thick sequence near São João Baptista in the southwest part of Santiago (Fig. 1C) indicates that the lower part correlates with the Gauss Normal Polarity chron, whereas the upper part is constrained to the basal Matuyama Reversed Polarity chron (Knudsen et al., 2009). The Assomada and Monte das Vacas Formations were later suggested to be part of the same eruptive event, a post-erosional phase that took place between 0.7-1.5 Ma (Holm et al., 2008; Ramalho et al., 2010a, b). However, a better separation between the products of these formations, and between them and Pico da Antónia, is problematic and still needs to be addressed. Mapping by Serralheiro (1976) shows that the wave-cut basalt bench on which Darwin's rhodolith sequence rests corresponds to the Old Eruptive Complex on Santa Maria, whereas the pillow basalt and subaerial flows that buried Darwin's rhodolith beds represents the upper member of the Pico da Antónia Eruptive Complex. Other criteria suggest this sequence to be younger (as treated below).

2.3 Volcanostratigraphic setting of Darwin's rhodolith beds on Santiago

Darwin (1844, p. 1–2) described the Praia area as such: "the country, viewed from the sea, presents a varied outline: smooth conical hills of a reddish color (like Red Hill…), and others less regular, flat-topped, and of a blackish color (…) rise from successive step-formed plains of lava". Effectively, the SE corner of Santiago is characterized by a gentle slope interrupted by sparse, deep but wide canyons, young

volcanic cones and a few tabular hills. This morphology suggests a young volcanic landscape that contrasts greatly with the deeply incised morphology of the central portion of the island, where a more evolved relief is largely carved into the Pico da Antónia Eruptive Complex and its precedent units (Fig. 3A). Not surprisingly, the seemingly young morphology of SE Santiago presents stronger affinities with the Assomada plateau (Fig. 3A), a valley-filling post-erosional volcanic sequence that dominates the central western area of the island, and dated around 0.7 – 1.1 Ma (Serralheiro, 1976; Holm et al., 2008; Barker et al., 2010). The landscape from Praia Baixo to Cidade Velha and inland to Rui Vaz reflects a fairly well preserved substructural surface of a lava shield where the only elevations standing above this surface correspond to contemporaneous or younger volcanic cones, or to older residual reliefs enclosed by the lava shield as areas of land completely surrounded by younger lava flows (Figs. 3B, C).

This younger sequence originated from a number of vents mainly located on the slopes of Serra do Pico da Antónia and extended all the way to the coast. Topographic highs correspond to the remains of the older and eroded Pico da Antónia volcano, the tops of which are remnants of its original surface. They can be used to reconstruct the approximate slope of this volcanic edifice, a surface that was about 70 m higher than the surrounding shield. The younger lava-shield sequence can be assigned to the Assomada Formation, complemented by lesser volumes of Monte das Vacas Formation, both of which erupted during the Late Pleistocene (Figs. 3B, C). The latter unit comprises cinder cones (e.g. Monte das Vacas) and a few lava flows that were either channeled by a drainage network precursory to the present-day network, or mantled the plateau's surface. A Pleistocene age for the sequence previously described is also supported by the 700 ka ±

200 ka age for the basalt flows on Ilhéu de Santa Maria in Praia harbor (Hebeda in Boekschoten and Best, 1988).

Coastal lava shields typically generate lava deltas, where flows enter the sea. These comprise a bottomset unit of underlying sediments and pillow breccias, a prograding foreset unit of pillow lavas and hyaloclastites, and a topset unit of flat-lying subaerial flows. The eruptive sequence previously described is no exception, and created some of the best lava delta structures that can be found in Cape Verde (Ramalho et al., 2010a). It is precisely at the base of these lava deltas (in the bottomset unit), overlying any of the precedent units, or between different delta generations, that most of the rhodolith-rich carbonate sediments described by Darwin occur (Fig. 3D).

3. Methods

Strip logs for stratigraphic sections were assembled along the SE shores of Santiago, modified after the standard format used by Shell Oil Company. Care was taken to register occurrences of trace fossils. Variations in rhodolith deposits were noted and representative examples were photographed. Samples collected for calcareous nannofossils were laterally replicated along the most fossiliferous, finer grained and less indurated layers in the carbonate succession where outcrop conditions allowed access to extended sections. Macrofacies indicated shallow coastal paleoenvironments rich in coarse bioclasts. Thus, the fine fractions from samples were concentrated in laboratory test tubes through overnight settling from a vigorously shaken half-sediment, half-tap-water suspension. The top fine fraction was extracted directly to a cover glass by a Pasteur pipette, spread into a rippled smear, and permanently mounted. Smear slides were

scanned for coccoliths on a petrographic microscope (Zeiss Ortholux II-Pol) at x1250 magnification along a 3-cm column (approximately 5 mm^2).

Whole rhodolith specimens from specific stratigraphic intervals were measured on site (to the nearest millimeter) across three principal axes (long, intermediate, and short). Data from these measurements were subjected to analysis based on the triangular plot among spherical, ellipsoidal, and discoidal shapes according to the format applied to rhodolith studies by Bosence (1976, 1983) as modified from Sneed and Folk (1958). A limited number of rhodoliths was retained for taxonomic studies using thin sections. Where possible, close attention was paid to finding the maximum thickness of the pillow basalt above each section studied in the carbonate succession.

On Maio Island (Cape Verde archipelago), the south shores were explored east from Vila do Maio over a distance of about 10 km for modern rhodolith deposits. Likewise, the north shores of Fuerteventura (Canary archipelago) were canvassed for modern rhodolith deposits along the coastal road between Corralejo and El Cotillo over a distance of 24 km. A quadrat with dimensions 0.5 x 0.5 m (0.25 m^2) also subdivided into 25 squares measuring 10 x 10 cm, was used to estimate the size, density, and overall numbers of rhodoliths washed onto beaches or trapped below sea cliffs. The surface area of over-wash deposits and berms was measured using a meter tape, as was the width of wave-cut platforms at various localities. An extensive photographic record was assembled to illustrate the natural range in variations of coastal rhodolith deposits.

4. Results

4.1 Stratigraphic analyses of Darwin's rhodolith sequence

Table 1 lists geographic co-ordinates and gives a summary of other basic information from 11 profiles that characterize sedimentary successions with extensive rhodolith materials exposed in sea cliffs along the SE coast of Santiago (Figs. 1C, D). Outcrops on the west side of Ilhéu de Santa Maria in the Praia harbor area are sufficient in lateral extent to log five stratigraphic sections spaced approximately 50 m apart with a crude north-south orientation (Figs. 1D, 4). Lithic sands derived from eroded basalt on Santa Maria declined through sections 1 and 5. Sedimentary structures include planar laminae, low-angle laminae (Fig. 5A), small-scale cross laminae, and hummocky cross-stratification (Fig. 5B). Calcareous content demonstrates an increase through upper strata in all but section 3, where the upper 3 m are covered. Section 3 also shows two levels with conglomerates. The lower conglomerate sits on an uneven basalt platform with up to 30 cm of relief. Scattered whole rhodoliths with basalt cores are included in this deposit and fragmented rhodoliths are pooled in depressions on the unconformity surface with a lower subaerial (a'a) lava flow. This flow is considered an early valley-filling extrusion from Monte das Vacas (Fig. 3B). The upper conglomerate includes a 1-m thick oyster mound with many oysters directly attached to basalt clasts. Above the mound, the conglomerate commonly includes the limpet *Patella* together with echinoid spines and scattered whole rhodoliths (Fig. 5C). Section 4 provides the thickest, most continuous sequence on the island and features an interval with conglomerate laterally equivalent to the upper conglomerate in section 3. Here, the interval includes *Patella* and *Conus*, as well as scattered whole rhodoliths, but is notably enriched by rhodolith fragments. Stringers with abundant whole rhodoliths are especially repetitive in strata above the conglomerate. Section 5 includes planar laminae low in the profile together with whole

rhodoliths exhibiting basalt cores (Fig. 5D). In contrast, this profile ends with elements of hummocky cross stratification (Fig. 5B), which are exclusive to section 5.

Volcanic rocks from the Monte das Vacas Formation on the west side of Ilhéu de Santa Maria consist of a'a lava flows laid down on a 25-cm to 35-cm thick basal clinker bed that can be traced for 150 m south from section 1 to section 4 (Table 1). The layer immediately above carbonate strata at section 5 is a peperite, showing evidence of direct contact between lava and wet sediments.

Stratigraphic profiles 6-8 are aligned with a northwest-southeast orientation along a distance of 1.35 km that extends from the edge of the Praia old-town plateau to the east side of the modern harbor, Porto da Praia (Fig. 1D). Section 6 (Fig. 6) is located at the foot of Travessa da Cruz Vermelha, a full kilometer almost due north of section 1 on Ilhéu de Santa Maria (Fig. 1D). The spatial relationship is noteworthy, because the lower 30 cm of section 6 includes a diverse fossil assemblage of marine gastropods dominated by *Turritella bicingulata* Lamark, packed in fine sand with mud rip-up clasts. The succession loses much of its lithic content above the 3.25-m level, where strata of sandy limestone take over. Stringers with whole rhodoliths and basalt pebbles are common at intervals through this part of the section. A distinctive red tuff follows and notably thickens laterally to the west. A thick a'a basaltic lava flow (or flows) covers the tuff.

Section 7 (Fig. 6) is exposed in a road-cut partly up the hill along the north side of Rua da Achada Grande in the Praia harbor area. The profile for this section features a robust basal conglomerate of well-rounded basalt cobbles and boulders sitting on an unconformity exhibiting up to 2 m of lateral relief with the Old Eruptive Complex.

Fragmented rhodoliths together with the molds of gastropods like *Strombus latus* Gmelin (= *S. bubonius* Lamark) and bivalves are scattered through the matrix.

The log for section 8 (Fig. 6) is based on a long exposure through the entire sedimentary sequence between the Old Eruptive Complex and the Assomada Formation. At the base, conglomerate consisting of basalt cobbles thinly scattered in a matrix of fine-to-medium lithic sand drapes a basalt shelf with up to 3 m of topographic relief. The matrix includes scattered whole rhodoliths. Fossil oysters are attached to some of the basalt cobbles. Fossil content is scarce through the ensuing 3.5 m of lime-rich sandstone, but includes rare oyster shells, cidaroid echinoid spines, crab claws, and the trace fossil *Bichordites* isp.. Near the top, a homogeneous limestone almost 2-m thick consists of about 80% rhodolith debris in which bands of small rhodoliths are common (Fig. 6). The trace fossil *Phycodes palmatus* (Hall) is common in the top few centimeters. The sedimentary succession is capped by a typical lava delta sequence comprising a foreset unit of pillow lavas, up to 12 m thick, and a topset unit of subaerial basalt flows. The volcanic structure indicates a paleowater depth of approximately 12 m. Section 8 is not as far south as section 1 on Ilhéu de Santa Maria, but the corner locality shares an east-west alignment with sections 9 and 10 at Portinho da Mulher Branca and section 11 on the east side of Ponta das Bicudas (Fig. 1D).

Sections 9 and 10 record thick, uninterrupted sequences less than 50 m apart (Figs. 1D, 7) that sit on an uneven surface on submarine flows that belong either to the Pico da Antónia Eruptive Complex, or more probably to an earlier lava delta sequence of the same Assomada Formation. The principal difference between the two profiles is that the basal conglomerate at section 9 is nearly three times as thick as that from section 10.

A peculiarity of the conglomerate in section 9 is the inclusion of a single, large and well-rounded limestone boulder. In both profiles, the overlying carbonate strata are notably homogeneous with minor mixing by lithic sands. Generally, section 10 is more rhythmic with recurrent fining-upward cycles from 10 cm – 20 cm in thickness that typically include bands of whole, small rhodoliths (Fig. 8). The upper few meters of section 9 include examples of swaley cross stratification, not found in section 10. Within the upper meter of both successions, good examples of trace fossils (*Dactyloidites ottoi* Geintz and *Skolithos* isp.) are prominent (Fig. 5E). Sections 9 and 10 are capped by a lava delta sequence, comprising a 12 – 15 m foreset unit of pillow lavas and a topset unit of flat-lying subaerial lava flows. The passage zone between the foreset and topset units marks the contemporaneous relative sea level, suggesting an equivalent paleowater depth.

The profile for section 11 from the east side of Ponta das Bicudas (Fig. 7), is based on exposures in a small limestone quarry showing an abutment unconformity between four distinct partially eroded pillow-mounds in the lower Assomada Formation and carbonate beds that rise landward through a vertical height of nearly 3 m over a lateral distance of 10 m. At this juncture, a 1.35-m high wall of basalt thinly encrusted with fossils of epilithic organisms marks the landward limit of the quarry. Basalt mounds lower in the quarry sequence are left projecting through the limestone, which often show halos of encrusting corals (*Siderastrea radians* Pallas) intact on the basalt. The lower limestone layers left around the basalt mounds typically include the trace fossil *Thalassinoides* isp., while upper layers feature the trace fossil *Dactyloidites* isp. In contrast, the vertical basalt face retains traces of the encrusting hydrozoan *Millepora alcicornis* (Linnaeus) in growth position, as well as scattered remains of barnacles

attributed to *Megabalanus* sp. and *Balanus* sp. and more seldom oysters. Here, the upper lava delta sequence of the Assomada Formation is represented by a thick succession of basalt pillows that sit directly on a flat bench of the lower submarine flows with barely a thin seam of encrusting *Millepora* in between. Typical pillow basalt sitting on carbonate strata are illustrated in Figure 4F a short distance north of section 11.

4.2 Calcareous nannofossil biostratigraphy

Most samples proved barren of calcareous nannofossils, but all contained common to abundant unidentifiable carbonate bioclasts of macroshells together with minute fragments (< 20 μm) of non-geniculate coralline algae. However, multiple samples from horizons at three localities (Fig. 1D, sections 3, 8, and 9) yielded results that allowed identification of coccolith assemblages. Three lateral subsamples collected 2.7 m above the base of section 6 at Travessa da Cruz Vermelha (Fig. 4) produced small *Gephyrocapsa* (*G. ericsonii-aperta* McIntyre and Bé) and *Reticulofenestra minuta* Roth. Eight lateral subsamples collected between 5.35 and 5.70 m about the base of section 8 at Porto da Praia, East (Fig. 3) yielded only *Gephyrocapsa* (*G. ericsonii-aperta*). Three lateral subsamples collected 5.25 m above the base of section 9 at Portinho da Mulher Branca (Fig. 6) gave the most diverse assemblage of calcareous nannofossils, including *Calcidiscus leptoporus* (Murray and Blackman) Loeblich and Tappan, *Gephyrocapsa oceanica* Kamptner, small *Gephyrocapsa* (*G. ericsonni-aperta*), *Reticulofenestra haqii-minutula* (Gartner) Haq and Berggren, and *Reticulofenestra minuta*.

The occurrence of small-size (≤ 3.5 μm) gephyrocapsids implies that the stratigraphic range of the fossiliferous carbonate units is clearly younger than mid Lower

Pliocene (mid Zanclean), because the first appearance of the genus is marked at biozone NN14 (Young in Bown, 1998; Nannotaxa) around 4 Ma. The presence of moderate-sized *Gephyrocapsa oceanica* suggests an age younger than 1.7 Ma (biozonal transition CN13a-CN13B) according to Raffi et al. (2006). The most recent species of coccolithophore to occur in the fossil record, *Emiliania huxleyi* Lohmann was not found.

4.3 Calcareous nannofossil taphonomy

There are two taphonomical reasons for layers with coastal macrofossil assemblages to be barren of calcareous nannofossils. The first is due to hydrodynamic conditions that may have prevented these micron-sized biogenic particles to settle after being carried by currents and waves from the open ocean. The second is post-depositional diagenetic dissolution. To minimize the possible effect of diagenetic carbonate lixiviation, samples were collected avoiding levels rich in volcanic debris, reddish color and/or fossil casts. However, the strata under consideration often outcrop as a strongly cemented limestone, as for example at Ponta das Bicudas. Here, the absence of calcareous nannofossils is clearly due to strong diagenetic recrystallization that also may distort coccoliths beyond recognition. The few horizons from sections that yielded calcareous nannofossils indicate that the assemblage is quite poor and with low diversity. Such characteristics are attributed to settling conditions unfavorable for micron-sized particles under near-shore conditions with high-energy hydrodynamics. Identified taxa mostly are represented by small forms that would be the first eliminated under diagenetic dissolution. Lower diversity assemblages dominated by opportunistic gephyrocapsids also suggest a coastal scenario. Absence of calcareous nannofossils in

the clay-rich sediments around the oyster mound on Ilhéu de Santa Maria (Fig. 4, section 3) is attributed to possible brackish lagoonal conditions rather than diagenesis.

4.4 Fossil rhodolith shape and size analyses

Samples of whole rhodoliths varying in number from 50 – 81 specimens were extricated for measurements from narrowly defined stratigraphic intervals in sections 2 and 4 on Ilhéu de Santa Maria (Fig. 4), as well as from section 8 at Porto da Praia (Fig. 6) and section 9 at Portinho da Mulher Branca (Fig. 7). In all four plots regarding fossil samples (Fig. 9, A – D), roughly half the points fall into the top triangular space for spherical shapes, whereas nearly all remaining points fall into the middle in the tier directly below. Spillover to other spaces within these plots is directed only slightly to the lower right, representing a minor tendency toward ellipsoidal shapes. The most diffuse spread of points is evident in the plot of rhodoliths from section 2 on Ilhéu de Santa Maria (Fig. 9A). Table 2 reveals that the average maximum (A-axis), intermediate (B-axis), and minimum (C-axis) diameters for specimens from sections 8 and 9 agree closely in all dimensions. On average, the samples from Ilhéu de Santa Maria (Fig. 9, A and B) are from 9 to 5 mm smaller in maximum diameter compared to the samples from Porto da Praia and Portinho da Mulher Branca (Fig. 9, C and D).

4.5 Modern rhodolith deposit, Maio Island

A sample of 84 modern rhodoliths was selected for measurements at the base of a sea cliff near Lagoa, approximately 6.7 km east of Vila do Maio on Maio Island in the Cape Verde archipelago (Fig. 1B). Rhodoliths from this sample were found concentrated

in an abutment deposit at the landward termination of an approximately 95-m wide wave-cut platform eroded in basalt. All rhodoliths were bleached white, indicating a death deposit. Nearby, some bleached rhodoliths were trapped in small tidal pools, but otherwise the wave-cut platform appeared to be free of rhodoliths or other shelly bioclasts. Few rhodoliths (10%) revealed a central basalt pebble and most showed no evidence of nucleation around bioclasts. Figure 9E gives the triangular plot for this sample, which essentially is identical in distribution to those of fossil rhodolilths from Porto da Praia and Portinho da Mulher Branca (Fig. 9, C and D) on Santiago Island. With regard to dimensions (Table 2), the modern rhodoliths from the abutment deposit on Maio are in-between the average sizes for the long, intermediate, and short axes in comparison with those of fossil rhodoliths from the four localities on Santiago Island. They are somewhat larger than the fossil rhodoliths sampled from Ilhéu de Santa Maria, but somewhat smaller than those from Porto da Praia and Portinho da Mulher Branca.

4.6 Modern rhodolith deposits, Fuerteventura Island

The east and north shores of Fuerteventura Island in the Canary archipelago (Fig. 2B, C) feature a range of taphonomic end-points with respect to rhodoliths and rhodolith debris, among which are those that resemble the abutment deposit from Maio Island in the Cape Verde archipelago. Table 3 lists six study sites on Fuerteventura and gives their geographic co-ordinates, as well as categorizes and quantifies the various kinds of depositional settings. At locality 1 on the east coast of Fuerteventura south of Fustes (Fig. 2B), a thin cover of basaltic sandstone mixed with rhodolith-calcarenite drapes a consolidated Holocene deposit of the same kind (Fig. 10A). Both deposits slope gently

seaward at the same low angle (< 9°). This is the La Hondura locality listed by Zazo et al. (2002, table 2) as beach rock and dated from 2.1 – 2.6 Ka.

A most remarkable contemporary rhodolith accumulation is the platform overwash deposit near Caleta del Bajo de Mejillones approximately 3 km west of Corralejo (Fig. 2C). The deposit forms a supratidal beach 120 m long and 10 m wide that sits above the landward termination of an extensive wave-cut platform exposed at low tide to a width of 130 m perpendicular to shore. The stranded rhodoliths are small (Fig. 10B), ranging from 10 to 30 mm in diameter with an average long axis of 19 mm (Table 2). A sample quadrat covering 0.25 m^2 registers a surface layer of 1,250 rhodoliths, which equates to 5,000 rhodoliths per square meter. It is estimated that the exposed beach surface amounts to approximately six million rhodoliths. Excavation of a shallow test pit revealed the presence of upper and lower rhodolith beds (each 5 cm thick) separated by a layer of rhodolith sand. A random sample of 95 rhodoliths from the surface was selected for measurements and shape analysis, the results of which are shown in Figure 9F. Similar to the plots for rhodoliths from Santiago and Maio, the rhodoliths from Caleta del Bajo de Mejillones are largely constrained to the upper, central parts of the plot, but spill over to adjacent areas in the lower right, representing an affinity toward somewhat ellipsoidal shapes. Among the various fossil and modern samples analyzed, these are the smallest rhodoliths encountered in the study (Table 2).

Another overwash deposit with rhodoliths comparable in size and shape to those at Caleta del Bajo de Mejillones occurs immediately northeast of the cove at Majanicho (Fig. 2), where transported rhodoliths form a distinct berm. The feature is approximately 150 m long by 9 m wide and rises 1.4 m above the landward termination of a wave-cut

platform (Fig. 10C). On the inner basalt platform near the beam, small tidal pools commonly are filled with bleached rhodoliths (Fig. 9D). In some cases, rhodoliths are locked in place by crystallized sea salt. Found only rarely at Caleta del Bajo de Mejillones and outside Majanicho, traces of brown algae anchored to the rhodoliths remain intact. This phenomenon, where the attachment of foliose algae to the rhodoliths acts to catch the wind, is known in Brazil as the "arribadas" (Dias and Villaça, 2012). It means that the rhodoliths originated in well-lighted waters where the brown algae thrive, but arrive seasonally on the beaches due to onshore winds that drag the rhodoliths along.

The inner cove at Majanicho shows more evidence of wrack lines with brown algae mixed with assorted rhodoliths. The wrack cover in bays farther west at Caleta de Beatriz and Caleta del Marrajo (Fig. 2, localities 5 and 6) is even more extensive. At Playa Hierro (Fig. 2C, locality 4), an exposed beach facing northeast with an area not less than 1,500 m^2 is composed almost entirely of very coarse rhodolithic sand. Inland directly south of Caleta del Marrajo (Fig. 2C, locality 6), coarse to medium sand (0.25 – 1.0 mm in diameter) derived from finely crushed rhodoliths and minor lithics derived from basalt form a dune field coving 40,000 m^2 (Fig. 9E, F). Persistent trade winds transport beach sand inland, the southerly direction confirmed by asymmetrical ripples.

4.7 Rhodolith taxonomy

Taxonomic identification is based on axial petrograhic thin sections prepared from samples collected at selected horizons in profiles 2 and 4 on Ilhéu de Santa Maria and profile 9 at Portinho da Mulher Branca. Preliminary analysis indicates that a combination of taxa is common in the fossil material. That is, a given rhodolith specimen

is dominated by *Sporolithon* sp., but also includes secondary colonization by one of two species from the Family Hapalidiaceae, in addition to rare *Lithophyllum* sp. One rhodolith sample from stratigraphic profile 4 (Fig. 4) was entirely dominated by a species from the Family Hapalidiaceae. Regarding modern rhodoliths collected from Maio (Cape Verde archipelago) and Fuerteventura (Canary archipelago), the taxonomy is far more limited. Preliminary analysis suggests that a single taxon of uniformly small rhodoliths belonging the Family Hapalidiaceae, possibly *Lithothamnion* sp., is represented among the over-wash deposits that crossed extensive wave-cut platforms on the southwest coast of Maio Island (Fig. 9E) and the north shores of Fuerteventura (see Table 2).

5. Discussion

5.1 Darwin's geology and geomorphology reappraised

Judged against the standard of field studies typical for the early 1800s, Darwin's working methods were sound (Herbert, 2005), but some of his interpretations changed with time (Pearson and Nicholas, 2007). Several aspects of Darwin's matured observations on "St. Jago" in the Cape Verde archipelago stand out as astute, while others are less incisive. The initial chapter of *Geological Observations on the Volcanic Islands* (Darwin, 1844, p. 1) introduces a map showing many of the physical features around SE Santiago, including an arc of six hills (labeled A-F) rising inland between 1.5 and 3 km from the coast, as well as two small volcanic craters closer to the coastline. These volcanic hills were interpreted by Darwin as formerly part of an inland plateau that encircled more of the island at the same elevation, now dissected in part by stream erosion but also isolated by subsequent basalt flows. Essentially, Darwin correctly

envisioned a geomorphologic feature that later entered the lexicon from the Hawaiian word kipuka, meaning an elevated area surrounded by lava flows. He also related the craters at Red Hill (Monte Vermelho) and Signal Post Hill (Facho) to the source of volcanic flows associated with the burial of calcareous strata in the rhodolith sequence along the coast. His observation is correct because these sites contributed flows that partially mantled the coastal plateau, however, the bulk of the lava shield probably flowed from sources further inland, as the uphill continuity of the shield surface suggests.

Darwin (1844, p. 4) explicitly stated that the white calcareous layers with "Nulliporae" must have "accumulated in a shallow sea, near an ancient coastline." He also emphasized that the calcareous deposit is notable for its extreme regularity. Elsewhere, Darwin (1844, p. 7) qualified the relationship by stating that the contact between the upper layers of the deposit and overlying basalt marks a conspicuous boundary that is "nearly horizontal." He posited that when observed in ravines that intersect the coast, the calcareous strata dip seaward "probably with the same inclination as when deposited round the ancient shores of the island." Moreover, the changing attitude of abutment unconformities at the base of the succession is clearly shown by the rolling nature of the lower contact with up to several meters of paleotopography exposed in cross section along a distance of nearly 1 km west of the ravine at Portinho da Mulher Branca (Fig. 3F). In effect, the surface of marine onlap imitates at a smaller scale the same kind of topography developed at higher elevations in the landscape illustrated by Darwin's six volcanic hills. Had they been inundated by a more extensive marine transgression, those hills would form headlands along an evolving coastline. The thickest carbonates signify the infilling of sediments in drowned inlets to small coastal valleys.

In contrast, basalt flows that define the unconformity at the top of the carbonate succession truly are remarkable for their evenness. Darwin (1844, p. 6) was perceptive in differentiating between lava that "in rolling over the sedimentary deposit at the bottom of the sea, has caught up large quantities of calcareous matter" as opposed to surface flows on "Quail Island" that left behind "vertical fissures" divided into "five-sided plates (Darwin 1844, p. 10). Today, the former are described as (submarine) pillow basalt (Fig. 4F), in contrast to the latter as columnar (subaerial) basalt. Most surprising, Darwin's insight was highly advanced regarding the pressurization of gas laced with carbonic acid released by submarine basalt flows in contact with carbonate sediments (peperite).

5.2 Interpretation of coastal paleogeography

The rhodolith beds studied by Darwin are overlain by parts of the Assomada Formation cropping out in sections 7 – 11. At Ilhéu de Santa Maria, the southern parts of the continuous carbonate outcrop (sections 3 – 5) are deposited between subaerial flows of the younger Monte das Vacas Formation. Darwin's paleoshore, thus, represents two different transgressions developed at approximately 1.1 – 0.7 Ma. The two shorelines are reconstructed in Figure 11.

In terms of relative sea level, the first onlap progressed across a rather uneven surface, as found to the east (Figs. 6 and 7, sections 7 through 11). This indicates rapid submergence without the erosion of a wave-cut platform that is more typically planar and laterally co-extensive. In terms of volcaniclastic input, cobbles and pebbles of basaltic origin are common in all studied profiles, near the base. A basal conglomerate was eroded as the ocean onlapped the volcanic edifice. The presence in section 9 (Fig. 7) of a

single, rounded limestone boulder with maximum visible diameter of 45 cm attests to an earlier transgression and deposition of limestone, but it is the sole indication of this earlier phase found in the eastern parts of the study area.

Profiles 8 –11 show an initial coarsening-upward pattern indicative of beach progradation. A shallow nearshore facies is found in this lower part. The profile from section 9 at Portinho da Mulher Branca lacks this near-shore facies and, thus, was likely to have accumulated in a slightly more distal position relative to shore. The upper part of sections 8 – 11 and the entire section 7 display a similar fining-upward succession that signals renewed transgression. Section 9 terminates with storm-generated structures showing swaley-cross-stratification (SCS) most commonly formed in an open-marine depositional environment below beach deposits but well above storm-wave base (Dumas and Arnott, 2006). This interpretation agrees well with the distal position postulated above. Section 7 is the only profile measured inland, 175 m from shore and 25 m above present sea level. It is a short sequence only 90 cm thick with a locally uneven basal unconformity. Due to its more upland position, marine onlap was delayed.

The second marine transgression advanced over smoother, subaerial a'a lava creating a wave-cut platform at the base of the only complete profile on Ilhéu de Santa Maria (Fig. 4, section 3). This transgression is recorded in sections 1 – 6. Sedimentary structures generally are scarce in the profiles, mainly due to bioturbation. Planar laminae are found in the lower parts of profiles on Ilhéu de Santa Maria together with a typical near-shore fauna. This represents deposition in a foreshore setting. Sections 1 – 3 on Ilhéu de Santa Maria commonly exhibit structures in the upper parts, such as low-angle cross stratification and ripples typical of the shoreface. Outboard, section 5 displays

hummocky-cross-stratification (HCS) at the top of the profile. This structure is normally produced in a position seaward of swaley-cross-stratification in a setting close to storm wave base (Dumas and Arnott, 2006). Section 5 is the most distal profile on the island, but has sediments with planar lamination and a near-shore assemblage similar to that found in the lower parts of the other sections on the island immediately underlying the HCS. In exceptional cases, HCS is reported from settings as shallow as the surf zone and the foreshore. It is possible that HCS of the anisotropic type noted by Dumas and Arnott (2006) represents such an exception in this section.

The same nearshore mollusks like *Strombus latus*, *Patella* sp., *Fisurella* sp., *Thais* sp., *Tellina* sp. together with crab claws are even more prevalent in the younger sequences 1 – 6 than in the older sequences. Oysters developed a small bioherm on Ilhéu de Santa Maria (section 3) and occur scattered through sediment in other profiles.
A cobble layer occurring higher in sections 3 and 4 on Ilhéu de Santa de Maria (Fig. 4), may be interpreted as a mass-flow deposit into a near-shore setting related to one of the frequent flash flood events that occur in arid volcanic islands.

Travessa da Cruz Vermelha (Fig. 6, section 6) is the most near-shore profile. It exhibits a high percentage of volcanic lithics all through the sequence. The amount of lithics decreases with distance from section 6, due south towards Ilhéu de Santa Maria. The profile at Travessa da Cruz Vermelha accumulated in a foreshore to shoreface position in a protected bay with a river, very similar to the landscape today. A similar trend in the lower parts of the section from high fine lithic content at Porto da Praia (Fig. 6, section 8) to virtually no lithic content at Pontas das Biscuda (Fig. 7, section 11) attests to the existence of a river-fed bay in roughly the same position also during the first of two

transgressions. In all profiles, the lithic content in limestone strata near the top of the succession is very low to non-existent. Therefore, a reasonable conclusion is that marine onlap drowned the local source of clastic materials.

5.3 Interpretation of trace fossils

Trace fossils are most apparent in the eastern profiles from Porto da Praia to Ponta das Bicudas (Figs. 6 and 7, sections 8 – 11). The only exception is at Travessa da Cruz Vermelha (Fig. 4, section 6), where the only trace fossil observed was *Paleophycus* isp., known to appear in environments from non-marine to marginal, shallow or deep marine settings (Buatois et al., 2002; MacEachern et al., 2007). *Bichordites* isp. occurs in lithic sands within the lower parts of section 8 (Porto da Praia) compared with the other profiles. According to Bernardi et al. (2010), *Bichordites* is typical of an environmental transition from a fully marine setting to a near-shore, brackish environment. Farther east, the most common trace fossil in the lower and shallowest parts of profiles 9 – 11 is *Thalassinoides* isp. This trace fossil typically appears in shallow marine environments from littoral to open platform settings (Buatois et al., 1996, 2002; MacEachern et al., 2007). Collectively, the trace fossils indicate a terrestrial source near the area of present-day Cidade da Praia, but with gradually more open-marine conditions further east.

Phycodes isp. appears in the middle part of the profiles at Portinho da Mulher Branca. It also is present in the upper parts of Porto da Praia, East, where it is represented by *Phycodes palmatus*. This trace fossil is considered a good indicator of shallow-marine to brackish environments (Singh et al., 2008). It is cited from settings in the lower shoreface (Mángano and Buatois, 1994) and from tidal flats (Mángano and

Buatois, 2004). Abbassi (2007) mentions that *Phycodes* only occurs in relatively consolidated sediments associated with low-energy, shallow-marine environments. However, it also has been reported from non-marine, brackish water and deep-marine environments (Han and Pickerill, 1994). In the profile for section 8, *P. palmatus* occurs together with patellid gastropods, also indicative of shallow, near-shore conditions. Other indicators from section 9 at Portinho da Mulher Branca suggest a slightly more distal position. However, *Phycodes* isp. is coincidental with an incursion of fine lithic sediment from the west. This may mean that local fresh-water streams had some influence this far eastward during deposition of the middle and upper parts of the profile.

Dactyloidites isp. appears in the upper parts of sections 8 – 11 towards the east, with the species *Dactyloidites ottoi* near the top of sections 8 and 9. It is typically found in siliciclastic sandstones rich in plant debris from high- to moderate-energy, shallow-marine transitional environments. The distribution of *D. ottoi* is thought to be controlled by the sandy nature of the substrate and the presence of detrital plant remains. Aguirrezabala and Gibert (2004) cite it from fluvial-dominated deltas having high and discontinuous sedimentation rates with a paleodepth between 0 and 3 m.

5.4 Insights from rhodolith taphonomy

Rhodoliths are both geographically widespread (Foster, 2001) and broadly arrayed through the geological column (Aguirre et al., 2010). Thus, it is surprising that little attention previously has been paid to the potential insights afforded by rhodolith taphonomy. Lenses with rhodolith material are common in the shoreface Pleistocene deposits on Ilhéu de Santa Maria. Most occur in mud-rich, poorly sorted sandstone.

However, the lower parts of section 5 are analogous to the beds of crushed and well-sorted debris found exposed at low tide on the east coast of Fuerteventura at La Hondura (Fig. 10A). Lenses with whole rhodoliths occur in the lower, near-shore parts of Santiago Pleistocene sections 2, 5, 6, and 10 (Fig. 10). These were deposited in foreshore to shoreface settings, where they became buried as part of a general transgression. The base of section 4 on Ilhéu de Santa Maria features small tidal pools that trapped rhodoliths and rhodolith debris, as seen at the modern rock platforms on Maio and Fuerteventura islands (10D). Rhodolith stringers are even more common in the uppermost transgressive parts of the profiles together with abundant rhodolith debris (sections 2, 4, 6, 8, 9 and 10). At Portinho da Mulher Branca (section 9), some rhodoliths are incorporated in beds with swaley cross stratification. Clearly, these rhodoliths were transported across the open shelf during storm surges.

The only place where fossil rhodoliths appear to be preserved in depositional settings close to where they lived is from the middle part of Section 10 at Portinho da Mulher Branca. There, the older paleo-coast (Fig. 11) followed a series of small, south to southeast facing headlands and bays. The two sections studied at Portinho da Mulher Branca (Fig. 7) are different from one another, despite the short distance between them. Locations on opposite sides of a small bay are interpreted as the exposed side for section 9 and the leeward side for section 10. Major storms originated off the coast of Africa, much as today (Johnson et al., 2011). Storm-waves came either directly from the southeast or were reflected around Ponta da Bicudas to impact the western side of the little paleobay. Thus, section 9 is likely to have absorbed the brunt of storm energy. The thick basal conglomerate in section 9 was formed under strong wave action. In contrast,

only scattered boulders float in sediment at the base of section 10, formed under the relative shelter of the paleobay's leeward flank.

Storm energy dissipated rapidly with impact on the rocky headlands between Porto da Praia and Portinho da Mulher Branca, where fine sediments were deposited on the leeward sides. Section 10 (Figs. 7, 11) represents one such leeward setting, where 11 rhythmic fining-upward cycles are recorded. Each cycle consists of a thin stringer of rhodoliths near the base in coarse biocalcarenites overlain by a fining-upwards interval of 5 to 10 cm. The rhodolith stringers can be traced 30 m laterally further east where they bank against the basalt cliff face (Fig. 8). This scenario implies successive generations of rhodoliths living sheltered within the bay and being killed off by the fall-out from each successive major storm. The rhodoliths could not have been transported with the storms from offshore, because they would have been piled up in a wedge-shaped abutment against the cliff face.

The schematic diagram in Figure 12 summarizes rhodolith taphonomy in many of its potential endpoints. Rhodoliths swept off banks by persistent coastal currents on the east or west sides of island shelves in the Cape Verde and Canary archipelagos are presumed to contribute to bathyal deposits below the photic zone, and eventually are destined to dissolution at the carbonate-compensation depth below 5,000 m. High-energy events such as major storms or hurricanes are responsible for moving rhodoliths across wave-cut platforms and into the supratidal zone (Johnson et al., 2011, 2012). Normally, storm beds indicated by swaley and hummocky cross-stratification are formed under wave-surge conditions that lead to basin-ward transport. From our analysis, more spherical rhodoliths (Fig. 9) were susceptible to transport. Theoretically, tsunamis

represent events capable of carrying rhodoliths and rhodolith debris far inland. Along the coast north of Signal Post Hill, an unusually large block of rhodolith limestone (2.5 m x 1.20 m x 0.80 m thick) was deposited 70 m above sea level well above the stratum from which it originated. Lesser disturbances are more common and less energetic, but also responsible for depositing rhodolith material in storm beds (swaley and hummocky cross-stratification) as observed in profiles for sections 5, and 9, (Figs. 4 and 7). Modern storms also generate rhodolith beach and berm deposits (Figs. 9A, B, C). Dune deposits composed largely of fine rhodolith debris (Figs. 10E, F) are the result of persistent onshore winds, as in the stiff winds that blast the north and eastern shores of islands in the Cape Verde and Canary archipelagos. The only previously documented rhodolith sand dune is known from Isla Coronados in the Gulf of California (Sewell et al., 2007), but comparable occurrences are the predicted result of beach deflation by persistent onshore winds along the east and north sides of older islands lacking high rocky shores like Maio or Sal in the Cape Verde archipelago.

6. Conclusions

Several advances are demonstrated over the classic work by Darwin on Santiago Island regarding former rocky shores that were volcanic in origin and remained volcanically active on an intermittent basis.

1. The general age surmised by Darwin for the Santiago sequence was Cenozoic. Based on small-size ($\leq 3.5\ \mu$m) gephyrocapsid nannofossils, the onset of carbonate deposition in the succession can be correlated not prior than biozone NN14 (Lower Pliocene, upper Zanclean). Moreover, the occurrence of moderate-sized

Gephyrocapsa oceanica implies an age younger than 1.7 Ma (biozonal transition CN13a-CN13B) according to Raffi et al. (2006). Thus, Darwin's carbonate deposits are entirely Pleistocene in age.

2. Darwin clearly recognized that carbonate strata in the Santiago sequence represent the marine onlap of a former rocky shoreline. Although he developed a sophisticated sense of the island's present-day geomorphology, he did not fully appreciate the nature of the uneven unconformity between basalt bedrock and overlying limestone facies that covered a series of small headlands. Changes in lateral facies are subtle, but reflect definitive variations in closely spaced profiles.
3. Darwin was more impressed by the even continuity of the unconformity between the limestone and succeeding basalt flows, which he correctly differentiated between subaerial flows that cooled as columnar basalt and submarine flows formed as pillow basalt. Subaerial volcanics directly succeed carbonates in the western part of the district on Ilhéu de Santa Maria and the Old Town plateau. Based on local geomorphologic relationships and position within subaerial flows, these carbonates are interpreted as being somewhat younger than those to the east. Thick pillow basalts typically laced with sublimated carbonates succeed limestone strata east of the harbor area extending to the southeast side of the island. Maximum thickness of the pillow basalts suggests that the minimum water depth reached by submarine flows in this area was as much as 18 m.
4. The Pleistocene shorelines in southeast Santiago Island mimic the present coast with a similar sheltered embayment near the Old Town plateau and a slightly smaller peninsula at Ponta das Bicudas. A small stream emptied into the paleobay, as today,

confirmed by the amount of fine volcaniclastic sand and silt delivered to the most northern of the 11 profiles (Travessa da Cruz Vermelha). A minor progradation of terrestrial sediments widely interrupted coastal onlap, as detected in the lower parts of several profiles. The distal profile on the east side of Ponta das Bicudas registers a significant change in facies with the prominence of rock-encrusting corals. This implicates long-shore currents swept by northeasterly winds, much as today.

5. The carbonate succession is dominated by rhodolith materials, particularly in the upper parts where they account for as much as 80% by volume. Analysis of whole fossil rhodoliths shows a high selectivity for spherical rhodoliths over more discoidal or ellipsoidal growth shapes. Exceptionally, these were culled and transported during storm events. Rhodoliths thrived on relatively sheltered banks off the southeast coast of Santiago, where wave refraction from the northeasterly winds provided sufficient energy to keep them in motion under fair-weather conditions.
6. Rhodolith taphonomy studied from Recent deposits provides a useful means for comparison with fossil deposits of all ages. Older volcanic islands with low coastal topography and extensive wave-cut platforms feature a wide range of settings with rhodoliths and rhodolith materials captured in tidal pools and platform over-wash deposits, as well as beach, berm, hurricane, tsunami, and coastal dune deposits.

Acknowledgments

This endeavor was funded under grant CGL2010-15372-BTE from the Spanish Ministry of Science and Innovation to project leader Eduardo Mayoral (University of Huelva). Financial support to A. Santos came from the Spanish Ministry of Science and

Technology (Juan de la Cierva subprogram, Ref: JCI-2008-2431). Support by the Junta de Andalucía (Spanish government) to the Research Group RNM316 (Tectonics and Palaeontology) also is acknowledged. Extra support for work on calcareous nannofossils came from PTDC/MAR/102800/2008. Partial funding to Ledesma-Vazquez on this project came from the Programma Integral de Fortalecimiento Institucional 2010. The authors are grateful to António Serralheiro and José Madeira (Universidade de Lisboa) and to Alberto da Mota Gomes (Universidade de Cabo Verde) for providing bibliographic references, cartographic material, and general remarks on Cape Verde geology. Esther Martín González and Carolina Castillo (La Laguna University, Canary Islands) provided help and expert guidance on Fuerteventura Island. Riosmena-Rodríguez (Universidad Autónoma de Baja California Sur, La Paz, Mexico) kindly provided the generic identifications for fossil and Recent rhodoliths. A review by Davide Bassi (Università di Ferrara) helped to improve the final contribution.

References

Abbassi, N., 2007. Shallow marine trace fossils from Upper Devonian sediments of the Kuh-E Zard, Zefreh Area, Central Iran. Iranian Journal of Science and Technology, Transaction A, 31, 23 – 33.

Agirrezabala, L. M., Gibert J. M., 2004. Paleodepth and Paleoenvironment of *Dactyloidites ottoi* (Geinitz, 1849) from Lower Cretaceous Deltaic Deposits (Basque-Cantabrian Basin, West Pyrenees). Palaios 19, 276 – 291.

Aguirre, J., Perfectti, F., Braga, J.C., 2010. Integrating phylogeny, molecular clocks, and the fossil record in the evolution of coralline algae (Corallinales and Sporolithales, Rhodophyta). Paleobiology 36, 519 – 533.

Barker, A.K., Holm, P.M., Peate, D.W., Baker, J.A., 2009. Geochemical stratigraphy of submarine lavas (3 – 5 Ma) from the Flamengos Valley, Santiago, southern Cape Verde Islands. Journal of Petrology 50, 169 – 193.

Barker, A.K., Holm, P.M., Peate, D.W., Baker, J.A., 2010. A 5 million year record of compositional variations in mantle sources to magmatism on Santiago, southern Cape Verde archipelago. Contributions to Mineralogy and Petrology 160, 133 – 154.

Bassi, D., Nebelsick, J.H., Checconi, A., Hohenegger, J., Iryu, Y., 2009. Present-day and fossil rhodolith pavements compared: Their potential for analyzing shallow-water carbonate deposits. Sedimentary Geology 214, 74 – 84.

Bassi, D., Nebelssick, J.H., 2010. Components, facies and ramps: Redefining Upper Oligocene shallow water carbonates using coralline red algae and larger foraminifera (Venetian area, northeast Italy). Palaeogeography, Palaeoclimatology, Palaeoecology 295, 258 – 280.

Basso, D., 1998. Deep rhodolith distribution in the Pontian Islands, Italy: A model for the palaeoecology of a temperate sea. Palaeogeography, Palaeoclimatology, Palaeoecology 137, 173 – 187.

Basso, D., Nalin, R., Nelson, C.S., 2009. Shallow-water *Sporolithon* rhodoliths from North Island (New Zealand). Palaios, 24: 92 – 103.

Bernardi, M., Boschele, S., Ferretti, P., Avanzini, M., 2010. Echinoid burrow *Bichordites monastiriensis* from the Oligocene of NE Italy. *Acta Palaeontologica Polonica* 55 (3), 479 – 486.

Boekschoten, G.J., Best, M.B., 1988. Fossil and recent shallow water corals from the Atlantic islands off western Africa. Zoologische Mededelingen Rijksmuseum van Natuurlijke Historie te Leiden 62, 99 – 112.

Bosence, D., 1976. Ecological studies on two unattached coralline algae from western Ireland. Palaeontology 19, 71 – 88.

Bosence, D.K.J., 1983. The occurrence and ecology of Recent rhodoliths –a review. In: Peryt, T.M. (Ed.), Coated Grains. Springer-Verlag, Berlin, pp. 217-224.

Bown, P., 1998. Calcareous Nannofossil Biostratigraphy. Chapman and Hall, Dordrecht, The Netherlands, 314 pp.

Buatois, L.A., Mángano, M.G., Aceñolaza, F., 1996. Icnofaunas paleozoicas en sustratos firmes no marinos: Evidencias del Pérmico de la Cuenca de Paganzo. Ameghiniana 33, 265 – 270.

Buatois, L.A., Mángano, M.G., Aceñolaza, F., 2002. Trazas Fósiles: Señales de comportamiento en el registro estratigráfico. Edición Especial Museo Paleontológico Egidio Feroglio, nº 2, 382 pp.

Carracedo, J.C., Day, H., S., Guillou, H.J., Rodríguez Badiola, E., Canas, J.A., Pérez Torrado, F.J., 1998. Hotspot volcanism close to a passive continental margin: the Canary Islands. Geological Magazine 135, 591 – 604.

Darwin, C., 1839. Journal and Remarks, 1832-1836. In: FitzRoy, R. (Ed.), Narrative of the Surveying Voyages of His Majesty's Ships Adventure and Beagle Between the Years 1826 and 1836, Volume 3, Henry Colburn, London, 615 pp.

Darwin, C., 1842. The Structure and Distribution of Coral Reefs, Being the First Part of the Geology of the Voyage of the Beagle, under the Command of Capt. FitzRoy, R.N. During the Years 1832 to 1836. Smith Elder & Co., London, 214 pp.

Darwin, C., 1844. Geological Observations on the Volcanic Islands Visited During the Voyage of the H.M.S. Beagle. Smith, Elder & Co., London, 175 pp.

Darwin, C. 1958. Autobiography – with original omissions restored; edited with appendix and notes by his grand-daughter, Nora Barlow. Collins, London, 253 pp.

Dias, G.T., Villaça, R.C., 2012. Coralline algae depositional environments on the Brazilian central southeastern shelf. Journal of Coastal Research 28, 270 – 279.

Dumas, S., Arnott, R.W.C., 2006. Origin of hummucky and swaley cross-stratification; the controlling influence of unidirectional current strength and aggradation rate. Geology 34, 1073 – 1076.

Foster, M.S., 2001. Rhodoliths: between rock and soft places. Journal of Phycology 37, 659 – 667.

Gutiérrez, M., Gasillas, R., Ferandez, C., Balogh;, K., Ahijado, A., Castillo, C., Colmenero, J.R., García-Navarro, E., 2006. The submarine volcanic succession of the basal complex of Fuerteventura, Canary Islands: A model of submarine growth and emergence of tectonic volcanic islands. Geological Society of America Bulletin 118, 785 – 804.

Halfar, J., Mutti, M., 2005. Global dominance of coralline red-algal facies: A response to Miocene oceanographic events. Geology 33, 481 – 484.

Han, Y., Pickerill, R. K., 1994. *Phycodes templus* isp. nov. from the Lower Devonian of northwestern New Brunswick, eastern Canada. Atlantic Geology 30, 37 – 46.

Herbert, S., 2005. Charles Darwin, Geologist. Cornell University Press, Ithaca, New York, 485 pp.

Holm, P.M., Grandvuinet, T., Friis, J., Wilson, J.R., Barker, A.K., Plesner, S., 2008. An 40Ar-39 study of the Cape Verde hot spot: Temporal evolution in a semistationary plate environment. Journal of Geophysical Research (Solid Earth) 113 (B8), B08201.

Johnson, M.E., Backus, D.H., Riosmena-Rodríguez, R., 2009. Contribution of rhodoliths to the generation of Pliocene-Pleistocene limestone in the Gulf of California. In: Johnson, M.E., Ledesma-Vázquez, J. (Eds.), Atlas of Coastal Ecosystems in the Western Gulf of California: Tracking Limestone Deposits on the Margin of a Young Sea. University of Arizona Press, Tucson, pp. 83-94.

Johnson, M.E., da Silva, C.M., Santos, A., Baarli, B.G., Cachão, M., Mayoral, E.J., Rebelo, A.C., Ledesma-Vázques, J., 2011. Rhodolith transport and immobilization on a volcanically active rocky shore: Middle Miocene at Cabeço das Laranjas on Ilhéu de Cima (Madeira Archipelago, Portugal). Palaeogeography, Palaeoclimatology, Palaeoecology 300, 113 – 127.

Johnson, M.E., Perez, D.M., Baarli, B.G., 2012. Rhodolith stranding event on a Pliocene rocky shore from Isla Cerralvo in the Lower Gulf of California (Mexico). Journal of Coastal Research 28, 225 – 233.

Knudsen, M.F., Holm, P.M., Abrahamsen, N., 2009. Paleomagnetic results from a reconnaissance study of Santiago (Cape Verde Islands): Identification of cryptochron C2r.2r-1. Physics of the Earth and Planetary Interiors 173, 279 – 289.

Lyell, C., 1830. Principles of Geology, Being and Attempt to Explain the Former changes of the Earth's Surface by Causes now in Operation. Volume 1, John Murray, London, 346 pp.

MacEachern, J.A., Pemberton, G., Gingras, M.K., Bann, K.L., 2007. The ichnofacies paradigm: A five-year retrospective. In: Miller, W., III (Ed.), Trace Fossils, Concepts, Problems, Prospects. Elsevier, Amsterdam, The Netherlands, pp. 52-77.

Mángano, M. G., Buatois, L. A., 1994. Trazas fósiles e icnofábricas en depósitos carbonáticos cretácicos, las Cuevas, Alta Cordillera de Mendoza. Ameghiniana 31, 55 –66.

Mángano, M G., Buatois, L. A., 2004. Ichnology of Carboniferous tide-influenced environments and tidal flat variability in the North and stratigraphic analysis, Geological Society, Special Publication 228, 157 – 179.

Matsuda, S, Iryu, Y., 2011. Rhodoliths from deep fore-reef to shell areas around Okinawa-jima, Ryukyu Islands, Japan. Marine Geology 282, 215 – 230.

Nalin, R., Nelson, C.S., Bassor, D., Massari, F., 2008. Rhodolith-bearing limestones as transgressive marker beds: fossil and modern examples from North Island, New Zealand. Sedimentology 55, 249 – 274.

Pearson, P.N., Nicholas, C.J., 2007. 'Marks of extreme violence': Charles Darwin's geological observations at St Jago (São Tiago), Cape Verde islands. In: Wyse Jackson, P.N. (Ed.), Four Centuries of Geological Travel: The Search for

Knowledge on Foot, Bicycle, Sledge and Camel. Special Publications Geological Society, London 287, 239 – 253.

Pereira Filho, G.H., Amado Filho, G.M., de Moura, R.L., Bastos, A.C., Guimarães, S.M.P.B., Salgado, L.T., Francini Filho, R.B, Bahia, R.G. Pinto Abrantes, D., Guth, A.Z. Brasileiro, P.S., 2012. Extensive rhodolith beds cover the summits of southwestern Atlantic Ocean seamounts. Journal of Coastal Research 28, 261 – 269.

Raffi, I., Backman, J., Fornaciari, E., Palike, H., Rio, D., Lourens, L., Hilgen, F., 2006. A review of calcareous nannofossil astrobiochronology encompassing the past 25 million years. Quaternary Science Reviews 25, 3113 – 3137.

Ramalho, R., Helffrich, G., Vance, D., Schmidt, D.N., 2010a. Tracers of uplift and subsidence in the Cape Verde Archipelago. Journal of Geological Society 167, 519 – 538.

Ramalho, R., Helffrich, G., Cosca, M., Vance, D., Hofmann, D., Schmidt, D.N., 2010b. Vertical movements of ocean island volcanoes: Insights from a stationary plate environment. Marine Geology 275, 84 – 95.

Robertson, A.H.F., 1984. Mesozoic deep-water and Tertiary volcaniclastic deposition of Maio, Cape Verde Islands: Implications for Atlantic paleoenvironments and ocean island volcanism. Geological Society of America Bulletin 95. 433 – 453.

Santos, E., Mayoral, E.J., da Silva, C.M., Cachão, M., Johnson, M.E., Baarli, B.G., 2011. Miocene intertidal zonation on a volcanically active shoreline: Porto Santo in the Madeira archipelago, Portugal. Lethaia 44, 26 – 32.

Serralheiro, A., 1976. A geologia da Ilha de Santiago (Cabo Verde). Boletim do Museu e Laboratorio Mineralógico e Geológico da Faculdade de Ciências 14, 157 – 369.

Sewell, A.A., Johnson, M.E., Backus, D.H., Ledesma-Vázquez, J., 2007. Rhodolith detritus impounded by a coastal dune on Isla Coronados, Gulf of California. Ciencias Marinas 33, 48 – 494.

Singh, R.H., Rodriguez-Tovar, F.J., Ibotombi, S., 2008. Trace Fossils of the Upper Eocene–Lower Oligocene Transition of the Manipur, Indo-Myanmar Ranges (Northeast India). Turkish Journal of Earth Sciences 17, 821 – 834.

Steiner, C., Hobson, A., Favre, P., Stampfli, G.M., Hernandez, J., 1998, Mesozoic sequence of Fuerteventura (Canary Islands): Witness of early Jurassic sea-floor spreading in the central Atlantic. Geological Society of America Bulletin 110, 1304 – 1317.

Steller, D.L, Riosmena-Rodríquez, R., Foster, M.S. 2009. Living rhodolith bed ecosystems in the Gulf of California. In: Johnson, M.E., Ledesma-Vázquez, J. (Eds.), Atlas of Coastal Ecosystems in the Western Gulf of California: Tracking Limestone Deposits on the Margin of a Young Sea. University of Arizona Press, Tucson, pp. 72-82.

Sneed, E.D., Folk, R.L., 1958. Pebbles in the lower Colorado River, Texas, a study in particle morphogenesis. Journal of Geology 66, 114 – 150.

Zazo, C., Goy, J.L., Hillaire-Marcel, C., Gillot, P.Y., Soler, V., González, J.H., Dabrio, C.J., Ghaleb, B., 2002. Raised marine sequences of Lanzarote and Fuerteventura revisited – a reappraisal of relative sea-level changes and vertical movements in the eastern Canary Islands during the Quaternary. Quaternary Science Reviews 21, 2019 – 2046.

Figure Captions

Fig. 1. A) Maps at various scales for islands in the Canary and Cape Verde archipelagos, B) Bathymetry around islands in the Cape Verde archipelago, after Holm et al. (2008), C) Santiago Island, and D) Coastal zone around the Praia district in southeastern Santiago Island showing location of study sites 1 – 11.

Fig. 2. A) Maps at various scales for islands in the Canary archipelago showing bathymetry, B) Fuerteventura Island in its entirety, C) and Details of the northern coast on Fuerteventura Island showing the location of study sites 2 – 6 between the towns of Corralejo and El Cotillo.

Fig. 3. A) Digital Elevation Model of Santiago with main localities cited in the text, B) Geological map implanted over DEM (modified from Serralheiro 1976), C) Geological cross section XY in map B evidencing the correlation between the geomorphology and the volcanostratigraphy, and D) Detailed cross section of zone Z in map C.

Fig. 4. Stratigraphic profiles from Ilhéu de Santa Maria across from the Praia harbor; inset shows locations. The scale for Udden-Wentworth values in grain-size shown at the base of each section is given in phi units. The key to symbols for lithology, sedimentary structures, and fossil content applies also to Figs. 5 and 6.

Fig. 5. Details showing sedimentary structures, macro-fossils, trace fossils, pillow basalt, and paleotopography from the Pleistocene succession in the Praia area of Santiago Island: A) Low angle cross-laminae from section 1 on Ilhéu de Santa Maria, scale = 10 cm, B) Swaley cross-stratification from section 5 on Ilhéu de Santa Maria, scale = 4 cm, C) Fossil limpet shell (left: *Patella* sp. and fossil coral (right: *Favia* sp.)

from section 3 on Ilhéu de Santa Maria, D) Fossil rhodoliths with basalt cores from section 5 on Ilhéu de Santa Maria, E) Trace fossils (upper range: *Dactyloidites ottoi* and lower range: *Skolithos* isp.) from section 9 at Portinho da Mulher Branca, F) Pillow basalt (hammer for scale) at the top of the carbonate succession near section 11 on the east side of Ponta das Bicudas, and E) Panoramic view west from Ponta das Bicudas towards Cidade da Praia showing the uneven paleotopography of the lower unconformity (crane to the upper left extends 5.5 m off the ground).

Fig. 6. Stratigraphic sections 6 – 8 from cliffs below Travessa da Cruz Vermelha in Cidade da Praia to the road cut east of Porto da Praia (Fig. 1D).

Fig. 7. Stratigraphic sections 9 – 11 from sea cliffs extending to the east shores of Ponta de Bicudas (Fig. 1D).

Fig. 8. Rhythmic bands of whole rhodoliths and rhodolithic debris banked against a former cliff line at section 10, Portinho da Mulher Branca (Fig. 1).

Fig. 9. Triangular plots showing the relative shapes of fossil and modern rhodoliths: A, B) Fossil sample from sections 2 and 4 on Ilhéu de Santa Maria, C) Fossil sample from section 8 at Porto da Praia, D) Fossil rhodoliths from section 9 at Portinho da Mulher Branca; E) modern sample from Lagoa on Maio Island, and F) modern sample from Caleta del Bajo de Mejillones on Fuerteventura Island.

Fig. 10. Taphonomic grades of transported rhodolith materials on Fuerteventura in the Canary archipelago: A) Recent beach sand on Holocene beach rock at La Hondura, scale showing 2 cm; B) Small whole rhodoliths mixed with basalt pebbles on the beach at Caleta del Bajo de Mejillones, scale 4 cm, C) Berm composed of whole and fragmented rhodoliths near Majanicho, building with water tank for scale; D)

Tidal pool filled with bleached rhodoliths near Majanicho, scale 4 cm (center); E) White dune sands derived mostly from rhodoliths inland from Caleta del Marrajo, figures for scale; and F) Close-up of dune sand with asymmetrical ripples, scale showing 2.5 cm. See Figure 2C for locations.

Fig. 11. Paleoshore during the initial stage of Pleistocene marine onlap in SE Santiago Island in the Cape Verde archipelago compared with a slightly younger onlap related to Ilhéu de Santa Maria (approximately 700 Ka) and the escarpment below the Travessa da Cruz Vermelha (section 6). Under both scenarios, an embayment somewhat smaller than today existed to the west and a somewhat smaller peninsular than presently found at Ponta das Bicudas anchored the coast to the east.

Fig. 12. Schematic diagram showing taphonomic grades for carbonate deposits dominated by rhodoliths and degraded rhodolith materials.

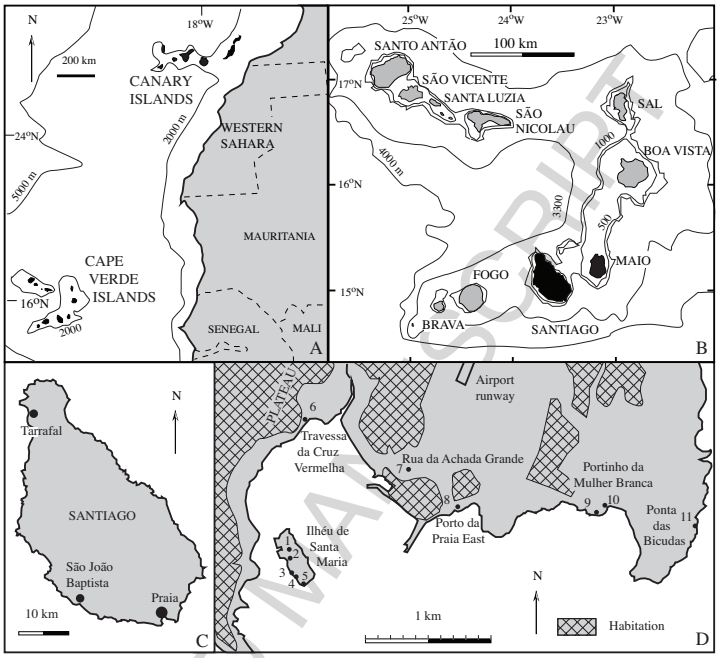

Fig. 1

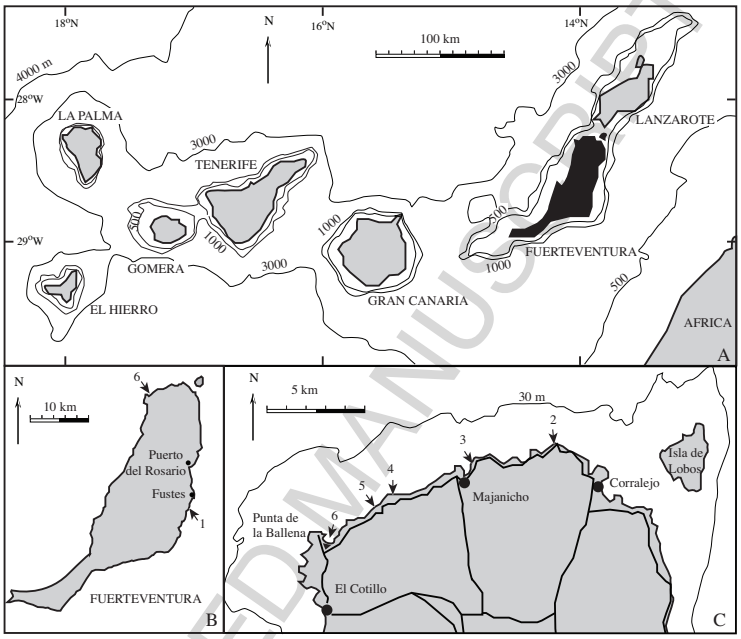

Fig. 2

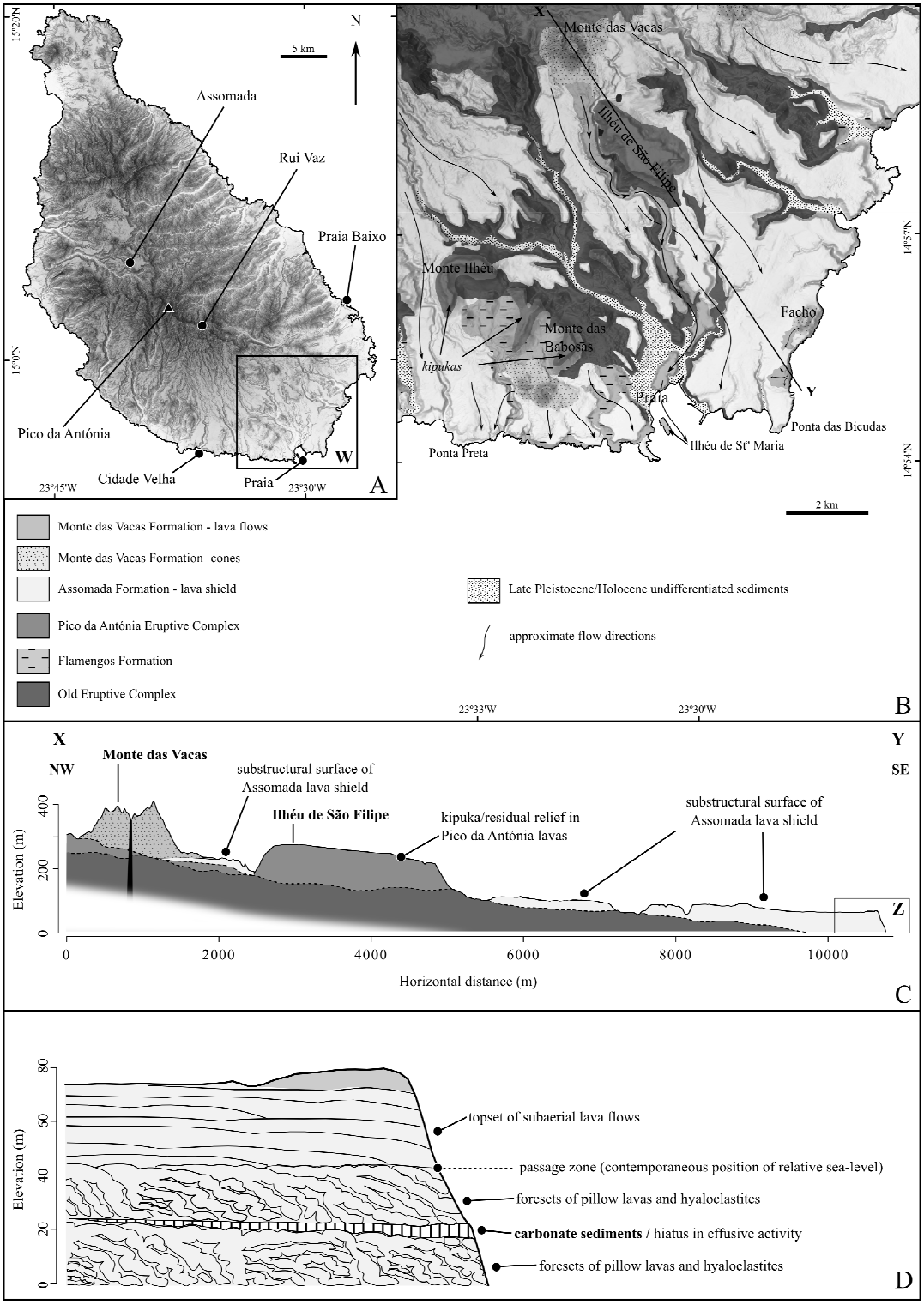

Fig. 3

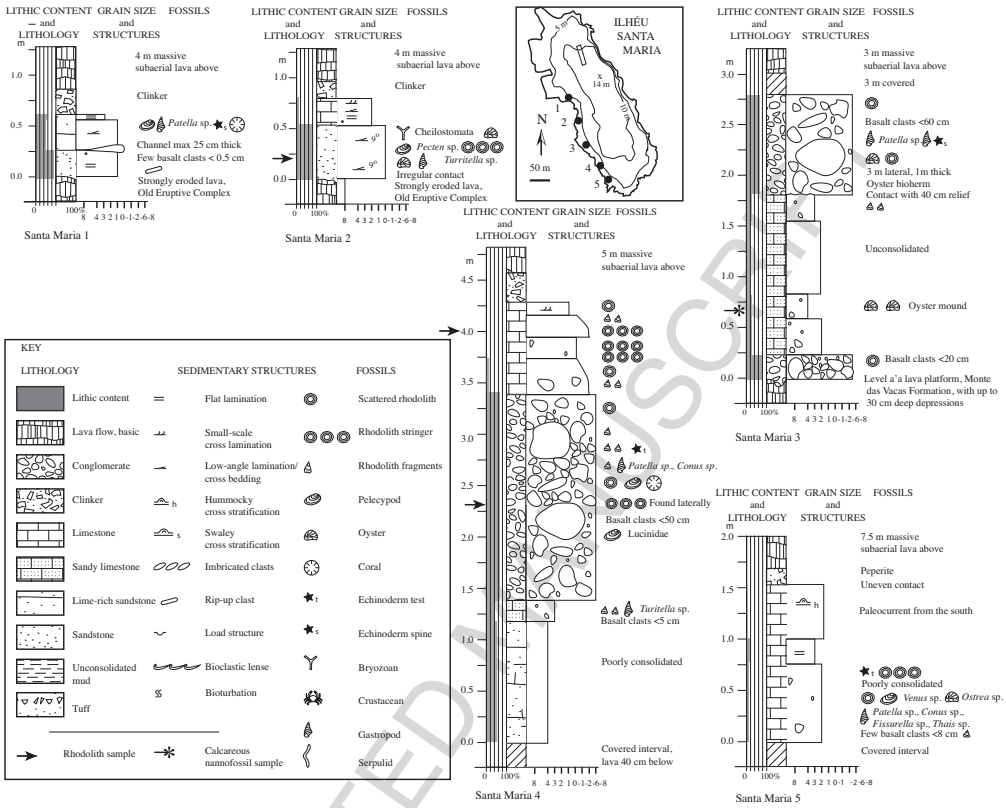

Fig. 4

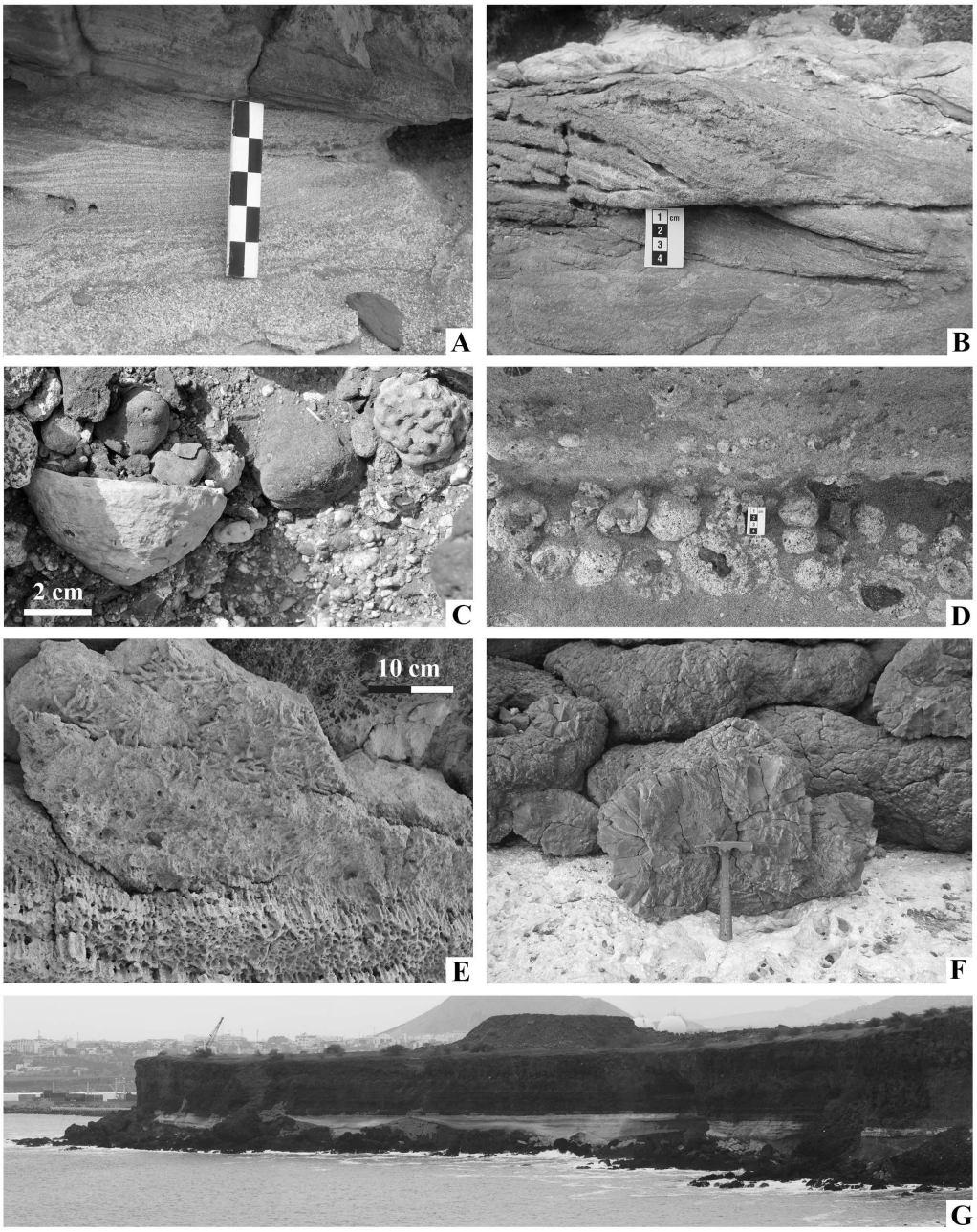

Fig. 5

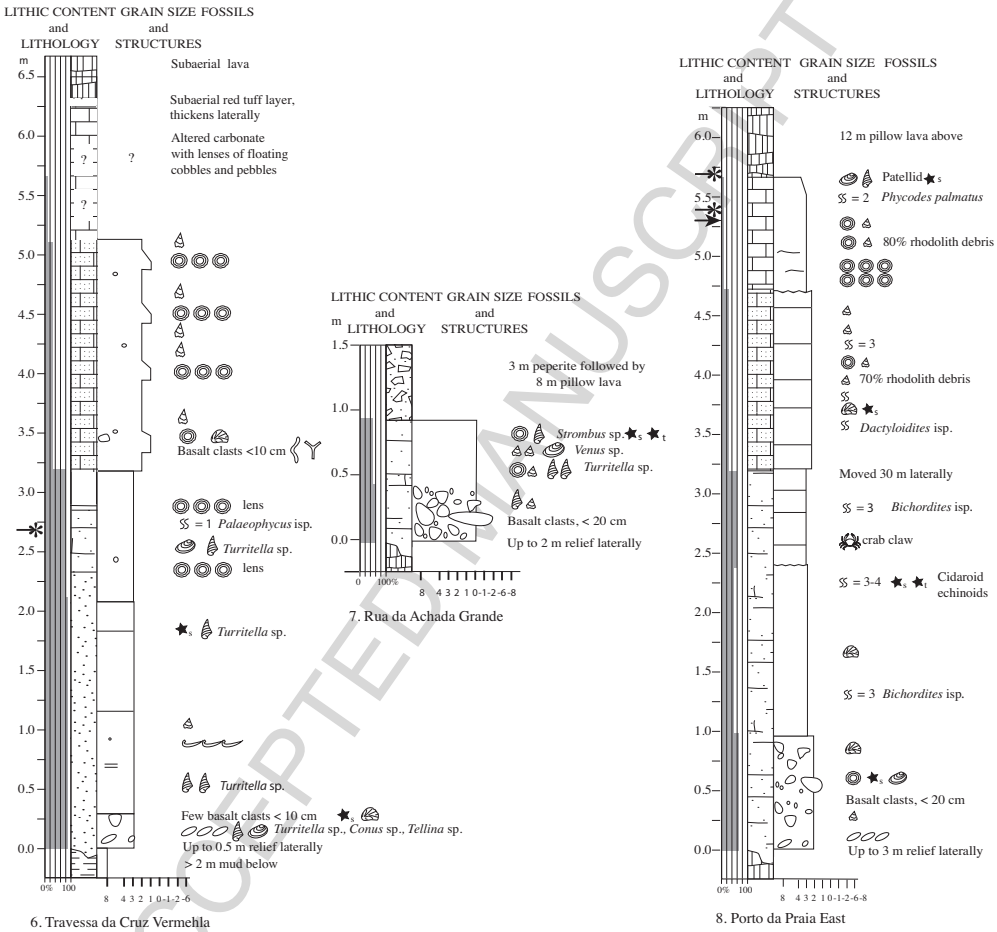

Fig. 6

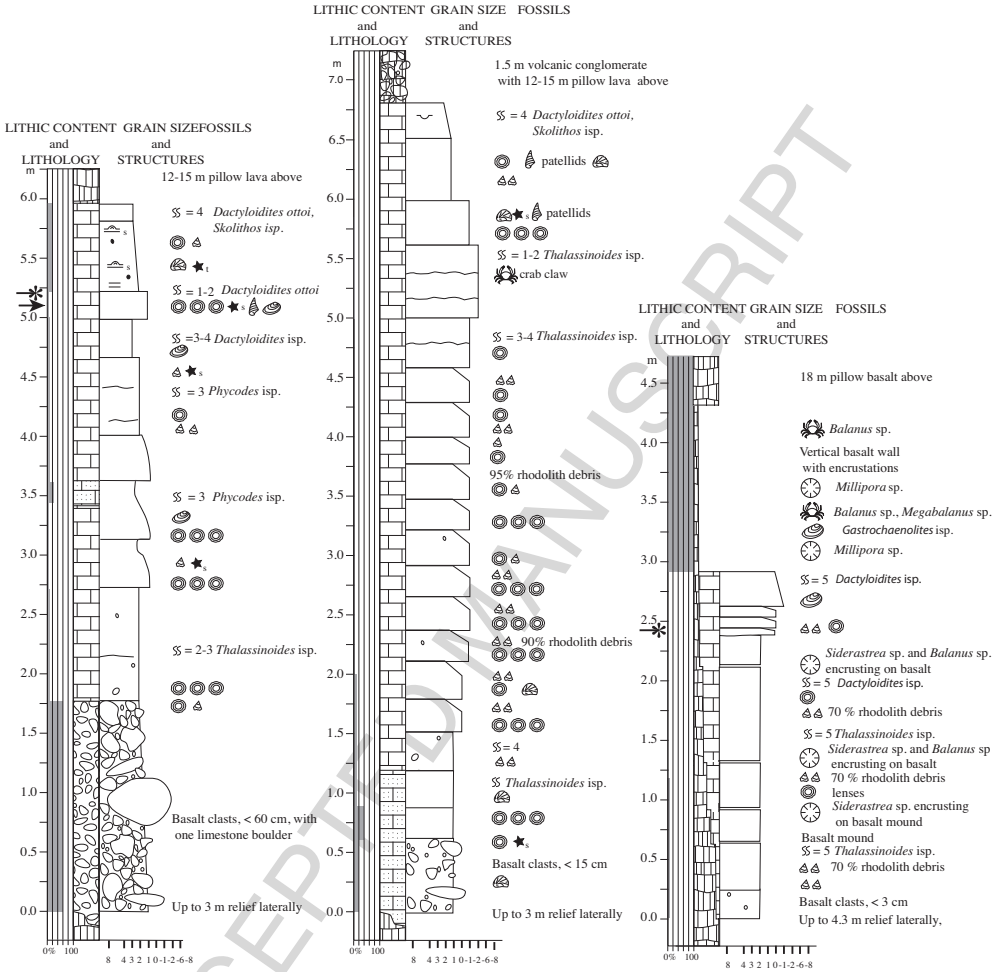

Fig. 7

Fig. 8

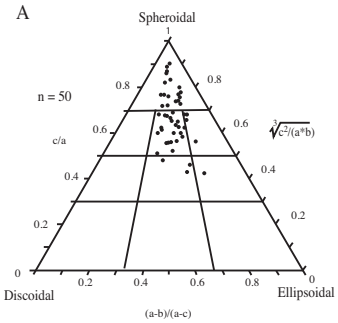

2. Santa Maria, 0.2 m above base

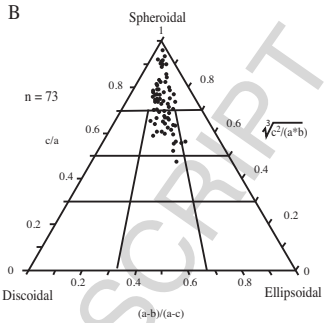

4. Santa Maria 2.3 m above base

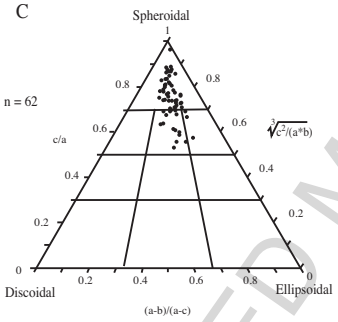

4. Santa Maria 4.0 m above base

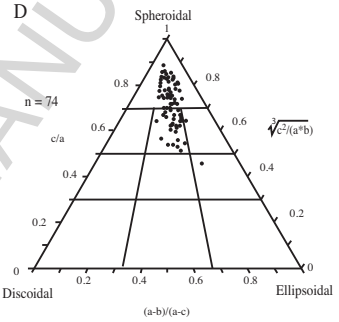

9. Portinho da Mulher Branca, 5.10 m above base

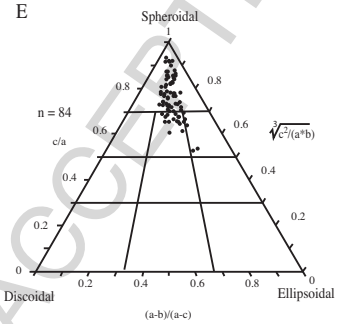

1. Lagoa do Barreiro, Maio

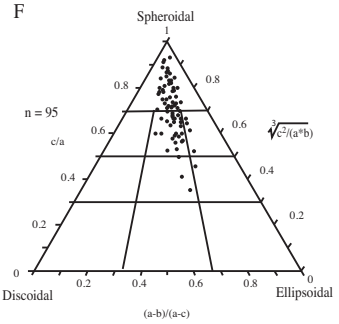

2. Bajo de Mejillones, Furteventura

Fig. 9

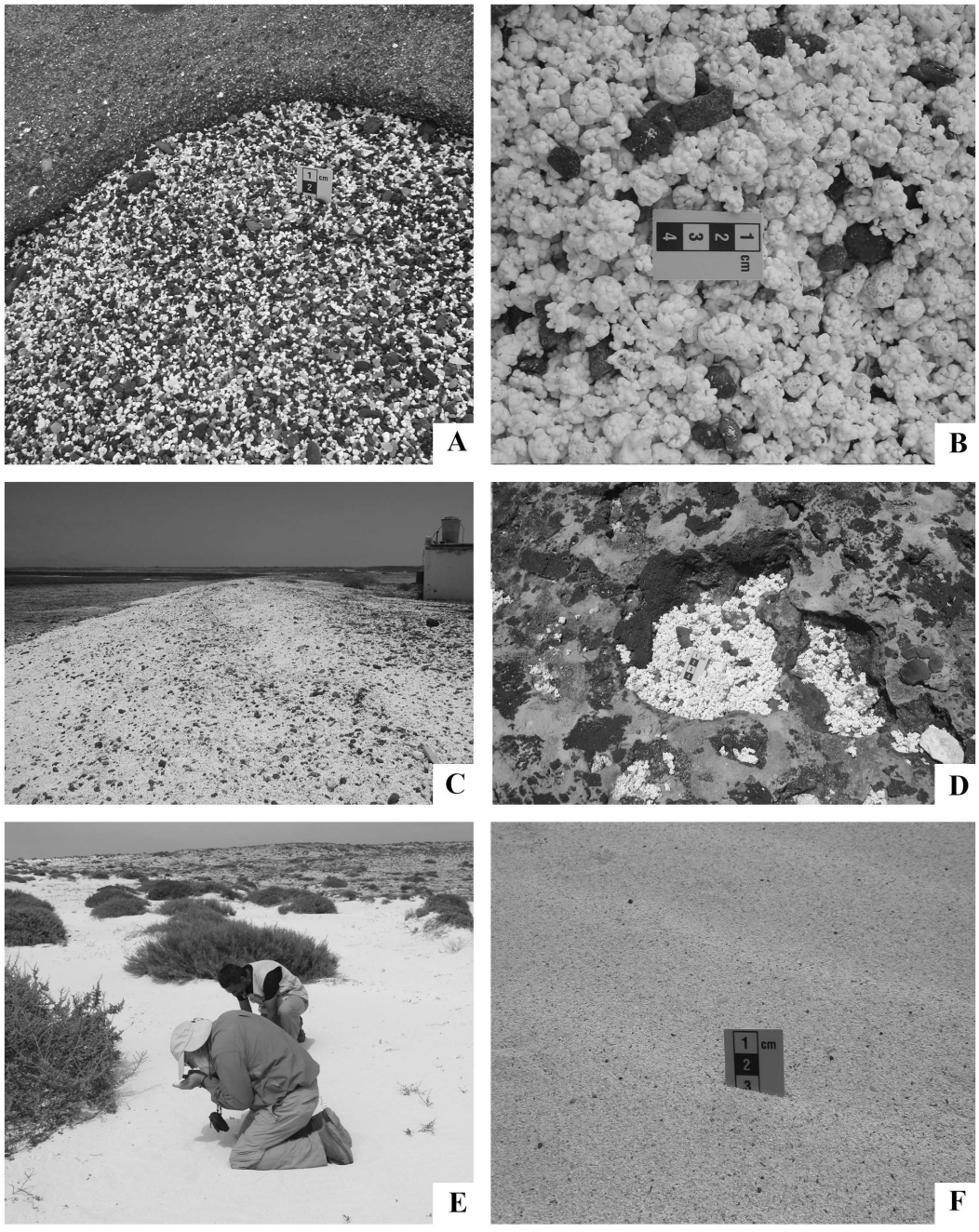

Fig. 10

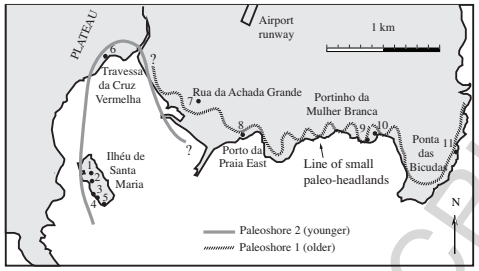

Fig. 11

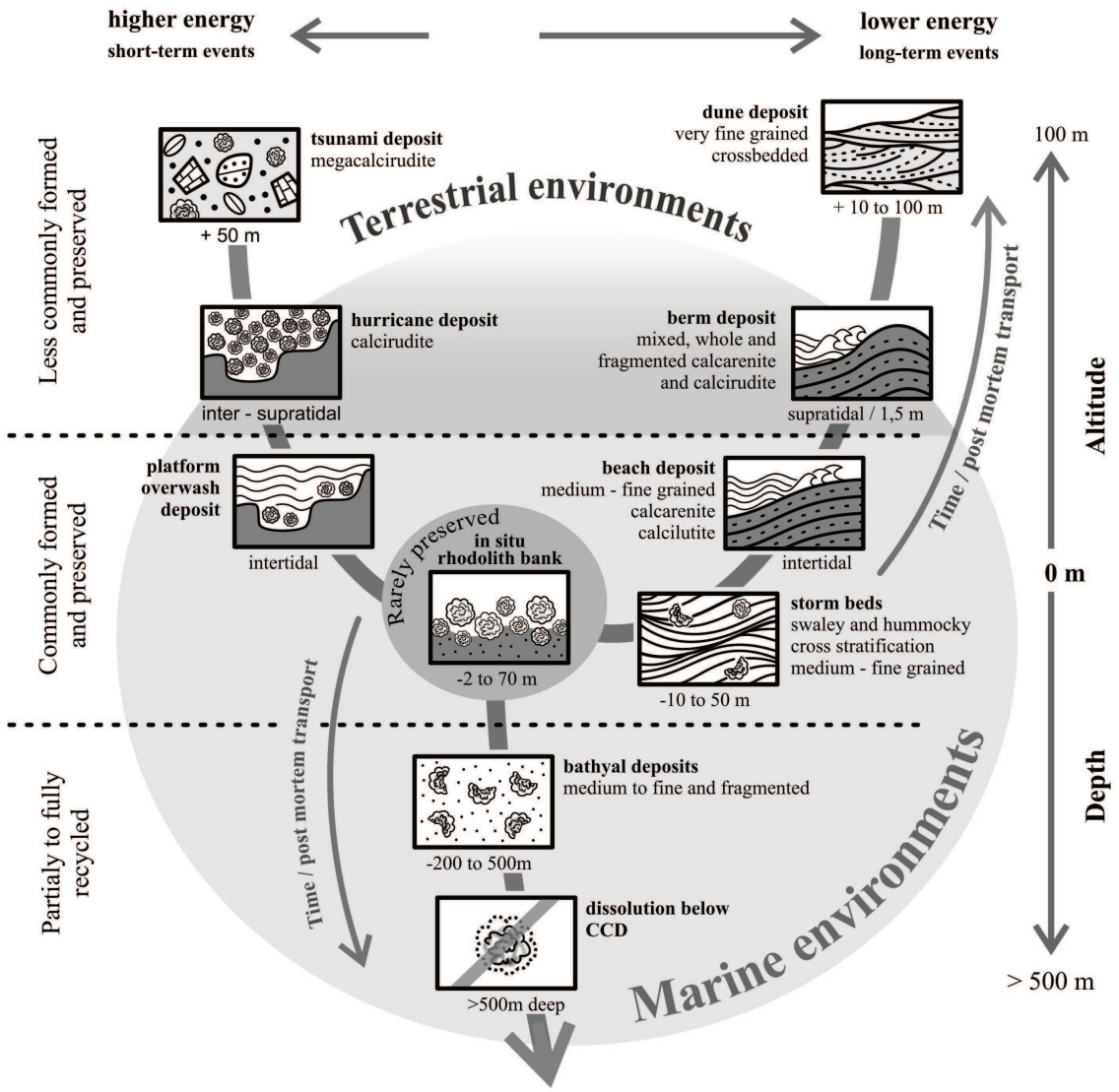

Fig. 12

Table 1. Geographic co-ordinates and other selected aspects from localities on the southeastern coast of Santiago Island (Cape Verde archipelago) where stratigraphic logs were measured in the rhodolith sedimentary succession

Locality name	Section number	Latitude	Longitude	Sediment strata (m)	Volcanic cover
Santa Maria, North	1	N14° 54' 22.79"	W23° 30' 29.31"	1.20	clinker
Santa Maria	2	N14° 54' 28.38"	W23° 30' 28.26"	0.80	clinker
Santa Maria	3	N14° 54' 23.52"	W23° 30' 26.82"	2.80	clinker
Santa Maria	4	N14° 54' 22.08"	W23° 30' 26.34"	4.70	clinker
Santa Maria, South	5	N14° 54' 20.52"	W23° 30' 24.60"	1.5+	peperite
T. Cruz da Vermelha	6	N14° 55' 01.14"	W23° 30' 24.72"	6.30	tuff
Rua da Achada G.	7	N14° 54' 47.98"	W23° 29' 56.65"	0.90	peperite
Porto da Praia, East	8	N14° 54'39.12"	W23° 29' 46.26"	5.60	pillow basalt
Portinho da Mulher Branca	9	N14° 54' 38.52"	W23° 29' 10.44"	5.90	pillow basalt
Portinho da Mulher Branca	10	N14° 54' 39.78"	W23° 29' 08.40"	6.80	pillow basalt
Ponta das Bicudas	11	N14° 54' 37.45"	W23° 28' 45.69"	3.00	pillow basalt

Table 2. Size variation in fossil rhodoliths (Praia area, Santiago Island, Cape Verde archipelago) and Recent rhodoliths (Maio Island, Cape Verde archipelago and Fuerteventura Island, Canary archipelago); standard deviation is shown only for the A-axis measurements

Location number and name	Total number sampled	Range of A-axis (mm)	Average A-axis (mm)	Standard deviation A (mm)	Average B-axis (mm)	Average C-axis (mm)
Santiago:						
2 Ilhéu Santa Maria	50	20 - 63	31.4	± 8.23	25.7	21.3
4 Ilhéu Santa Maria	73	17 - 69	33.8	± 10.04	28.4	24.5
8 Porto da Praia, East	81	17 - 84	40.2	± 12.06	33.8	28.7
9 Portinho da Mulher Branca	74	17 - 84	40.1	± 11.83	33.7	28.8
Maio:						
1 Lagoa	84	17 - 48	29.2	± 5.72	25.6	22.1
Fuerteventura:						
2 Bajo de Mejillones	95	10 -31	19.1	± 4.75	16.3	13.6

Table 3. Geographic co-ordinates and other selected features from localities on the east and north shores of Fuerteventura Island (Canary archipelago)

Locality name	Locality number	Latitude	Longitude	Type of deposit(s)	Area (m^2)
La Hondura	1	N28° 22' 27.89"	W13° 51' 59.91	Beach	5,000
Bajo de Mejillones	2	N28° 45' 08.80"	W13° 53' 55.01"	Platform overwash	1,200
Majanicho	3	N28° 44' 27.07"	W13° 56' 14.57"	Tidal pool; Berm	1,350
Playa el Hierro	4	N28° 44' 01.26	W13° 58' 29.46"	Outer beach	1,500
Caleta de Beatriz	5	N28° 43' 40.50"	W13° 58' 47.92	Inner-cove beach	1,200
Caleta del Marrajo	6	N28° 42' 39.36	W14° 00' 35.16"	Coastal dune	40,000